A two-level atom coupled to a two-dimensional supersymmetric and shape-invariant system: dynamics and entanglement

2007 J. Phys. A: Math. Theor. 40 3933

(http://iopscience.iop.org/1751-8121/40/14/012)

J. Phys. A: Math. Theor. **40** (2007) 3933–3957 doi:10.1088/1751-8113/40/14/012

A two-level atom coupled to a two-dimensional supersymmetric and shape-invariant system: dynamics and entanglement

A N F Aleixo[1] **and A B Balantekin**[2]

[1] Instituto de Física, Universidade Federal do Rio de Janeiro, RJ, Brazil
[2] Department of Physics, University of Wisconsin, Madison, WI 53706, USA

E-mail: armando@if.ufrj.br (Aleixo) and baha@physics.wisc.edu (Balantekin)

Received 4 December 2006, in final form 5 February 2007
Published 20 March 2007
Online at stacks.iop.org/JPhysA/40/3933

Abstract
A class of bound-state problems which represent the coupling of a two-level atom with a two-dimensional supersymmetric system involving two shape-invariant potentials was introduced in a previous paper. We study in this second paper the quantum dynamics and the entanglement for two models with different coupling Hamiltonians.

PACS numbers: 03.65.Fd, 03.65.Ge, 02.20.−a, 03.67.Mn

1. Introduction

In the first paper of this series [1] we introduced a class of coupled-channel problems consisting of a two-dimensional supersymmetric and shape-invariant system interacting with a two-level atom or molecule. Usually studied in the context of one-dimensional systems, supersymmetric quantum mechanics [2] deals with the partner Hamiltonians

$$\hat{H}_- = -\frac{\hbar^2}{2M}\frac{\mathrm{d}^2}{\mathrm{d}x^2} + V^{(-)}(x) = \hbar\Omega\hat{A}^\dagger\hat{A} \quad \text{and} \quad \hat{H}_+ = -\frac{\hbar^2}{2M}\frac{\mathrm{d}^2}{\mathrm{d}x^2} + V^{(+)}(x) = \hbar\Omega\hat{A}\hat{A}^\dagger \tag{1}$$

that can be written in terms of one-dimensional operators

$$\hat{A} \equiv \frac{1}{\sqrt{\hbar\Omega}}\left(W(x) + \frac{\mathrm{i}}{\sqrt{2M}}\hat{p}\right) \qquad \text{and} \qquad \hat{A}^\dagger \equiv \frac{1}{\sqrt{\hbar\Omega}}\left(W(x) - \frac{\mathrm{i}}{\sqrt{2M}}\hat{p}\right), \tag{2}$$

where $\hbar\Omega$ is a constant energy scale factor, introduced so that the operators $\hat{A}$ and $\hat{A}^\dagger$ are dimensionless, and $W(x)$ is the superpotential which is related to the potentials $V^{(\pm)}(x)$ via

$$V^{(\pm)}(x) = W^2(x) \pm \frac{\hbar}{\sqrt{2M}}\frac{\mathrm{d}W(x)}{\mathrm{d}x}. \tag{3}$$

A number of such pairs of Hamiltonians $\hat{H}_{\pm}$ share the integrability condition

$$\hat{A}(a_1)\hat{A}^{\dagger}(a_1) = \hat{A}^{\dagger}(a_2)\hat{A}(a_2) + R(a_1), \tag{4}$$

called shape invariance [3], where the parameter a_2 of the Hamiltonian is a function of its parameter a_1 and the remainder $R(a_1)$ is independent of the dynamical variables. In the cases studied so far the parameters a_1 and a_2 are either related by a translation [4, 5] or a scaling [6–10]. Supersymmetric quantum mechanics together with the shape invariance concept represents an elegant and powerful technique to investigate exactly solvable systems.

In earlier publications [11–13] we introduced a class of shape-invariant coupled-channel problems which generalize the Jaynes–Cummings Hamiltonian [14]. In this series of two papers we consider two different models which we call direct- and conjugate-coupled models to study the coupling of a two-dimensional supersymmetric and shape-invariant system with a two-level atom or molecule. For each model also we consider two possible forms of coupling: a standard coupling and an intensity-dependent coupling. The dynamics of this kind of coupled system is strongly dependent on the initial conditions, i.e., on the states in which the supersymmetric and shape-invariant potential systems and the atom are prepared at the beginning. In these circumstances we study in this second paper of the series the quantum dynamics of the models, analysing the evolution of some observable and investigating their consequences for the degree of entanglement of the coupled system.

The organization of the paper is as follows: in section 2 we present the Hamiltonian for the direct- and conjugate-coupled models and obtain its time-evolution operators and the density operators; in section 3 we obtain the temporal behaviour of the population inversion factor and the coupling potentials partial entropy; in section 4 we apply our generalized results for three different kinds of pairs of shape-invariant potentials (namely two harmonic oscillators, a harmonic oscillator plus a Pöschl–Teller potential and a harmonic oscillator plus a self-similar potential) discussing the relevant aspects of the time behaviour of each observable. Conclusion and brief remarks are given in section 5.

2. Direct- and conjugate-coupled systems

2.1. Hamiltonians

We consider in this study three interacting systems consisting of a single two-level atom or molecule simultaneously coupled with two shape-invariant potentials systems $V_x^{(\pm)}(x)$ and $V_y^{(\pm)}(y)$ which are associated with the operators $\hat{A}_x$ and $\hat{A}_y$, respectively. The Hamiltonian for this coupled system in the resonant case can be written in the form $\hat{H}_{\xi}^{(\mathrm{X})} = \hat{H}_0^{(\mathrm{X})} + \hat{\mathcal{V}}_{\xi}^{(\mathrm{X})}$, where its supersymmetric non-interacting part for the *direct-coupled model*, specified when $\mathrm{X} = \mathrm{D}$, is given by

$$\hat{H}_0^{(\mathrm{D})} = \hbar\Omega\left\{\left(\hat{A}_x\hat{A}_x^{\dagger} + \hat{A}_y\hat{A}_y^{\dagger}\right)\hat{\sigma}_+\hat{\sigma}_- + \left(\hat{A}_x^{\dagger}\hat{A}_x + \hat{A}_y^{\dagger}\hat{A}_y\right)\hat{\sigma}_-\hat{\sigma}_+\right\}. \tag{5}$$

The Hamiltonian $\hat{\mathcal{V}}_{\xi}^{(\mathrm{D})}$ for the *usual* and the *nonlinear interaction* cases, specified respectively when $\xi = \mathrm{U}$ and $\xi = \mathrm{N}$, is assumed with the forms

$$\hat{\mathcal{V}}_{\xi}^{(\mathrm{D})} = \hbar g\begin{cases}\hat{A}_x\hat{A}_y\hat{\sigma}_+ + \hat{A}_x^{\dagger}\hat{A}_y^{\dagger}\hat{\sigma}_-, & \xi = \mathrm{U};\\ \hat{A}_x\hat{A}_y\sqrt{\hat{N}_x\hat{N}_y}\hat{\sigma}_+ + \sqrt{\hat{N}_x\hat{N}_y}\hat{A}_x^{\dagger}\hat{A}_y^{\dagger}\hat{\sigma}_-, & \xi = \mathrm{N},\end{cases} \tag{6}$$

where g is a real constant coupling strength of the system, $\hat{N}_{x,y} = \hat{A}_{x,y}^{\dagger}\hat{A}_{x,y}$, and the two-level flip operators are defined by $\hat{\sigma}_{\pm} = \frac{1}{2}(\hat{\sigma}_1 \pm \mathrm{i}\hat{\sigma}_2)$, where $\hat{\sigma}_i$, for $i = 1, 2$ and 3, are the Pauli matrices.

For the *conjugate-coupled model*, specified when X = C, the total Hamiltonian components are defined as

$$\hat{H}_0^{(\mathrm{C})} = \hbar\Omega\left\{\left(\hat{A}_x\hat{A}_x^\dagger + \hat{A}_y^\dagger\hat{A}_y\right)\hat{\sigma}_+\hat{\sigma}_- + \left(\hat{A}_x^\dagger\hat{A}_x + \hat{A}_y\hat{A}_y^\dagger\right)\hat{\sigma}_-\hat{\sigma}_+\right\}, \tag{7}$$

while

$$\hat{\mathcal{W}}_\xi^{(\mathrm{C})} = \hbar g\begin{cases}\hat{A}_x\hat{A}_y^\dagger\hat{\sigma}_+ + \hat{A}_y\hat{A}_x^\dagger\hat{\sigma}_-, & \xi = \mathrm{U};\\ \hat{A}_x\sqrt{\hat{N}_x\hat{N}_y}\hat{A}_y^\dagger\hat{\sigma}_+ + \hat{A}_y\sqrt{\hat{N}_y\hat{N}_x}\hat{A}_x^\dagger\hat{\sigma}_-, & \xi = \mathrm{N}.\end{cases} \tag{8}$$

The nonlinear form in terms of the coupling potential operators $\hat{A}_x$ and $\hat{A}_y$ in the intensity-dependent interaction case ($\xi = \mathrm{N}$) stresses quantum effects in the time behaviour of the observable of the system [15, 16].

The algebraic formulation presented in [9] for shape-invariant systems can be applied in the Hamiltonian $\hat{H}_\xi^{(\mathrm{X})}$ by using the operators $\hat{B}_+^{(\alpha)} \equiv \hat{A}_\alpha^\dagger\hat{T}_\alpha$ and $\hat{B}_-^{(\alpha)} \equiv \hat{T}_\alpha^\dagger\hat{A}_\alpha$ defined with the introduction of the parameter translation operators $\hat{T}_\alpha \equiv \hat{T}_\alpha\big(a_1^{(\alpha)}\big)$ for each shape-invariant potential $V_\alpha^{(\pm)}(\alpha)$, where $\alpha = x$ or y. In these conditions the commutation relations $\big[\hat{B}_\mp^{(\alpha)}, \hat{B}_\pm^{(\beta)}\big] = \pm R_\alpha\big(a_0^{(\alpha)}\big)\delta_{\alpha\beta}$ and $\big[\hat{B}_\pm^{(\alpha)}, \hat{B}_\pm^{(\beta)}\big] = 0$, which traduce the shape-invariance condition (4) and the independence of the two potential systems, are satisfied. The final result can be written as $\hat{H}_\xi^{(\mathrm{X})} = \hat{\mathcal{T}}_\mathrm{X}\hat{h}_\xi^{(\mathrm{X})}\hat{\mathcal{T}}_\mathrm{X}^\dagger$ if we define the parameter translation inclusive operator for each model

$$\hat{\mathcal{T}}_\mathrm{D} = \hat{T}_x\hat{T}_y\hat{\sigma}_+\hat{\sigma}_- \pm \hat{\sigma}_-\hat{\sigma}_+ \qquad \text{and} \qquad \hat{\mathcal{T}}_\mathrm{C} = \hat{T}_x\hat{\sigma}_+\hat{\sigma}_- \pm \hat{T}_y\hat{\sigma}_-\hat{\sigma}_+ \tag{9}$$

and decompose the Hamiltonian $\hat{h}_\xi^{(\mathrm{X})}$ as $\hat{h}_\xi^{(\mathrm{X})} = \hat{h}_0^{(\mathrm{X})} + \hat{w}_\xi^{(\mathrm{X})}$, where

$$\hat{h}_0^{(\mathrm{X})} = \hbar\Omega\begin{cases}\big[\big(\hat{\mathcal{H}}_+^{(x)} + \hat{\mathcal{H}}_+^{(y)}\big)\hat{\sigma}_+\hat{\sigma}_- + \big(\hat{\mathcal{H}}_-^{(x)} + \hat{\mathcal{H}}_-^{(y)}\big)\hat{\sigma}_-\hat{\sigma}_+\big], & \mathrm{X} = \mathrm{D};\\ \big[\big(\hat{\mathcal{H}}_+^{(x)} + \hat{\mathcal{H}}_-^{(y)}\big)\hat{\sigma}_+\hat{\sigma}_- + \big(\hat{\mathcal{H}}_-^{(x)} + \hat{\mathcal{H}}_+^{(y)}\big)\hat{\sigma}_-\hat{\sigma}_+\big], & \mathrm{X} = \mathrm{C},\end{cases} \tag{10}$$

and with the Hamiltonian $\hat{w}_\xi^{(\mathrm{X})}$ for the two kinds of interactions given by

$$\hat{w}_\mathrm{U}^{(\mathrm{X})} = \hbar g\begin{cases}\big(\hat{B}_-^{(x)}\hat{B}_-^{(y)}\hat{\sigma}_+ + \hat{B}_+^{(x)}\hat{B}_+^{(y)}\hat{\sigma}_-\big), & \mathrm{X} = \mathrm{D};\\ \big(\hat{B}_-^{(x)}\hat{B}_+^{(y)}\hat{\sigma}_+ + \hat{B}_-^{(y)}\hat{B}_+^{(x)}\hat{\sigma}_-\big), & \mathrm{X} = \mathrm{C},\end{cases} \tag{11}$$

and

$$\hat{w}_\mathrm{N}^{(\mathrm{X})} = \hbar g\begin{cases}\big(\hat{B}_-^{(x)}\hat{B}_-^{(y)}\sqrt{\hat{\mathcal{H}}_-^{(x)}\hat{\mathcal{H}}_-^{(y)}}\hat{\sigma}_+ + \sqrt{\hat{\mathcal{H}}_-^{(x)}\hat{\mathcal{H}}_-^{(y)}}\hat{B}_+^{(x)}\hat{B}_+^{(y)}\hat{\sigma}_-\big), & \mathrm{X} = \mathrm{D};\\ \big(\hat{B}_-^{(x)}\sqrt{\hat{\mathcal{H}}_-^{(x)}\hat{\mathcal{H}}_-^{(y)}}\hat{B}_+^{(y)}\hat{\sigma}_+ + \hat{B}_-^{(y)}\sqrt{\hat{\mathcal{H}}_-^{(y)}\hat{\mathcal{H}}_-^{(x)}}\hat{B}_+^{(x)}\hat{\sigma}_-\big), & \mathrm{X} = \mathrm{C}.\end{cases} \tag{12}$$

We used the fact that $\hat{\mathcal{H}}_\pm^{(\alpha)} = \hat{B}_\mp^{(\alpha)}\hat{B}_\pm^{(\alpha)}$ and the unitarity property $\hat{T}_\alpha^\dagger\hat{T}_\alpha = \hat{T}_\alpha\hat{T}_\alpha^\dagger = \hat{1}$, where $\alpha = x$ or y.

2.2. Time-evolution operator and the state of the coupled system

By using the Hamiltonian $\hat{H}_\xi^{(\mathrm{X})}$ presented above we can write the Schrödinger equation for the coupled system as

$$\hat{H}_\xi^{(\mathrm{X})}\big|\Psi_\xi^{(\mathrm{X})}(t)\big\rangle = \mathrm{i}\hbar\frac{\partial}{\partial t}\big|\Psi_\xi^{(\mathrm{X})}(t)\big\rangle. \tag{13}$$

Defining the algebraic intrinsic wave state $\big|\psi_\xi^{(\mathrm{X})}(t)\big\rangle$ by $\big|\Psi_\xi^{(\mathrm{X})}(t)\big\rangle = \hat{\mathcal{T}}_\mathrm{X}\big|\psi_\xi^{(\mathrm{X})}(t)\big\rangle$ and using it in (13) we find

$$\hat{h}_\xi^{(\mathrm{X})}\big|\psi_\xi^{(\mathrm{X})}(t)\big\rangle = \mathrm{i}\hbar\frac{\partial}{\partial t}\big|\psi_\xi^{(\mathrm{X})}(t)\big\rangle, \tag{14}$$

where we considered that $\hat{H}_{\xi}^{(\mathrm{X})} = \hat{\mathcal{T}}_{\mathrm{X}}\hat{h}_{\xi}^{(\mathrm{X})}\hat{\mathcal{T}}_{\mathrm{X}}^{\dagger}$ and used the unitary property $\hat{\mathcal{T}}_{\mathrm{X}}\hat{\mathcal{T}}_{\mathrm{X}}^{\dagger} = \hat{\mathcal{T}}_{\mathrm{X}}^{\dagger}\hat{\mathcal{T}}_{\mathrm{X}} = \hat{1}$. Since the two terms of $\hat{h}_{\xi}^{(\mathrm{X})}$ satisfy the commutation relation $\big[\hat{h}_{0}^{(\mathrm{X})}, \hat{w}_{\xi}^{(\mathrm{X})}\big] = 0$, then writing the algebraic intrinsic wave state as

$$\big|\psi_{\xi}^{(\mathrm{X})}(t)\big\rangle = \exp\big(-\mathrm{i}\hat{h}_{0}^{(\mathrm{X})}t/\hbar\big)\big|\varphi_{\xi}^{(\mathrm{X})}(t)\big\rangle, \tag{15}$$

and using it in (14) we obtain

$$\hat{w}_{\xi}^{(\mathrm{X})}\big|\varphi_{\xi}^{(\mathrm{X})}(t)\big\rangle = \mathrm{i}\hbar\frac{\partial}{\partial t}\big|\varphi_{\xi}^{(\mathrm{X})}(t)\big\rangle. \tag{16}$$

Now introducing the time-evolution operator $\hat{U}_{\xi}^{(\mathrm{X})}(t,0)$ such as $\big|\varphi_{\xi}^{(\mathrm{X})}(t)\big\rangle = \hat{U}_{\xi}^{(\mathrm{X})}(t,0)|\varphi(0)\rangle$, where $|\varphi(0)\rangle$ is an arbitrary initial state and substituting this proposal into equation (16) it is possible to find

$$\hat{w}_{\xi}^{(\mathrm{X})}\hat{U}_{\xi}^{(\mathrm{X})}(t,0) = \mathrm{i}\hbar\frac{\partial}{\partial t}\hat{U}_{\xi}^{(\mathrm{X})}(t,0). \tag{17}$$

Since $\hat{w}_{\xi}^{(\mathrm{X})}$ is time independent the formal solution of (17) satisfying the initial condition $\hat{U}_{\xi}^{(\mathrm{X})}(0,0) = \hat{1}$ is

$$\hat{U}_{\xi}^{(\mathrm{X})}(t,0) = \exp\big(-\mathrm{i}\hat{w}_{\xi}^{(\mathrm{X})}t/\hbar\big). \tag{18}$$

Taking into account the series expansion of the exponential function, expressions (6) and (12) for $\hat{w}_{\xi}^{(\mathrm{X})}$ and using the properties of the $\hat{\sigma}_k$-operators in (18) it is possible to obtain the analytic expression of the time-evolution operator

$$\begin{aligned}\hat{U}_{\xi}^{(\mathrm{X})}(t,0) = {} & \hat{\sigma}_{+}\hat{\sigma}_{-}\cos\big(g\hat{\omega}_{\xi}^{(\mathrm{X})}t\big) + \hat{\sigma}_{-}\hat{\sigma}_{+}\cos\big(g\hat{\mu}_{\xi}^{(\mathrm{X})}t\big) \\ & + \mathrm{i}\hat{\sigma}_{+}\big[\sin(g\hat{\omega}_{\xi}^{(\mathrm{X})}t)\big]\hat{F}_{\xi}^{(\mathrm{X})} + \mathrm{i}\hat{\sigma}_{-}\big[\sin(g\hat{\mu}_{\xi}^{(\mathrm{X})}t)\big]\hat{G}_{\xi}^{(\mathrm{X})},\end{aligned} \tag{19}$$

where

$$\sqrt{\hat{\omega}_{\mathrm{N}}^{(\mathrm{D})}} = \hat{\omega}_{\mathrm{U}}^{(\mathrm{D})} = \sqrt{\hat{\mathcal{H}}_{+}^{(x)}\hat{\mathcal{H}}_{+}^{(y)}}, \qquad \sqrt{\hat{\mu}_{\mathrm{N}}^{(\mathrm{D})}} = \hat{\mu}_{\mathrm{U}}^{(\mathrm{D})} = \sqrt{\hat{\mathcal{H}}_{-}^{(x)}\hat{\mathcal{H}}_{-}^{(y)}}; \tag{20}$$

$$\sqrt{\hat{\omega}_{\mathrm{N}}^{(\mathrm{C})}} = \hat{\omega}_{\mathrm{U}}^{(\mathrm{C})} = \sqrt{\hat{\mathcal{H}}_{+}^{(x)}\hat{\mathcal{H}}_{-}^{(y)}}, \qquad \sqrt{\hat{\mu}_{\mathrm{N}}^{(\mathrm{C})}} = \hat{\mu}_{\mathrm{U}}^{(\mathrm{C})} = \sqrt{\hat{\mathcal{H}}_{-}^{(x)}\hat{\mathcal{H}}_{+}^{(y)}}, \tag{21}$$

and

$$\begin{aligned}\hat{F}_{\mathrm{U}}^{(\mathrm{D})} &= \hat{G}_{\mathrm{N}}^{(\mathrm{D})\dagger} = \hat{\beta}_{-}^{(x)}\hat{\beta}_{-}^{(y)}, \qquad \hat{G}_{\mathrm{U}}^{(\mathrm{D})} = \hat{F}_{\mathrm{N}}^{(\mathrm{D})\dagger} = \hat{\beta}_{+}^{(x)}\hat{\beta}_{+}^{(y)}, \\ \hat{F}_{\mathrm{U}}^{(\mathrm{C})} &= \hat{G}_{\mathrm{N}}^{(\mathrm{C})\dagger} = \hat{\beta}_{-}^{(x)}\hat{\beta}_{+}^{(y)}, \qquad \hat{G}_{\mathrm{U}}^{(\mathrm{C})} = \hat{F}_{\mathrm{N}}^{(\mathrm{C})\dagger} = \hat{\beta}_{+}^{(x)}\hat{\beta}_{-}^{(y)}\end{aligned} \tag{22}$$

with

$$\hat{\beta}_{\pm}^{(\alpha)} = \frac{1}{\sqrt{\hat{\mathcal{H}}_{\mp}^{(\alpha)}}}\hat{B}_{\pm}^{(\alpha)}, \qquad \alpha = x \text{ or } y. \tag{23}$$

With the expression of the time-evolution operator $\hat{U}_{\xi}^{(\mathrm{X})}(t,0)$ we can write down the final expression for the algebraic intrinsic wave state of the coupled system as

$$\big|\psi_{\xi}^{(\mathrm{X})}(t)\big\rangle = \exp\big(-\mathrm{i}\hat{h}_{0}^{(\mathrm{X})}t/\hbar\big)\hat{U}_{\xi}^{(\mathrm{X})}(t,0)|\varphi(0)\rangle, \tag{24}$$

which is still valid for any pair of shape-invariant potentials.

2.3. The density operator

A simple and elegant way of incorporating statistical distributions of initial conditions into quantum dynamics of the coupled system is to represent the state of the quantum system by using the Hermitian density operator, defined as $\hat{\rho}(t) = |\Psi(t)\rangle\langle\Psi(t)|$. At any time $t > 0$, the time evolution of the operator $\hat{\rho}(t)$ is given by the Liouville equation of motion $\mathrm{i}\hbar\,\mathrm{d}\hat{\rho}(t)/\mathrm{d}t = [\hat{H}(t), \hat{\rho}(t)]$, obtained from the density operator definition and the Hamiltonian $\hat{H}(t)$ of the system. Knowledge of $\hat{\rho}(t)$ enables us to obtain the expectation value of any observable $\hat{O}$ through

$$\langle\hat{O}(t)\rangle = \frac{\mathrm{Tr}(\hat{\rho}(t)\hat{O})}{\mathrm{Tr}(\hat{\rho}(t))}. \tag{25}$$

To apply the density operator formalism for our supersymmetric coupled problem we use the algebraic intrinsic state vector (24) to obtain

$$\begin{aligned} &\hat{\rho}_{\xi}^{(\mathrm{X})}(t) = \exp\left(-\mathrm{i}\hat{h}_0^{(\mathrm{X})}t/\hbar\right)\hat{U}_{\xi}^{(\mathrm{X})}(t,0)\hat{\rho}_{\mathrm{o}}\hat{U}_{\xi}^{(\mathrm{X})\dagger}(t,0)\exp\left(\mathrm{i}\hat{h}_0^{(\mathrm{X})}t/\hbar\right), \\ &\text{where} \qquad \hat{\rho}_{\mathrm{o}} = |\varphi(0)\rangle\langle\varphi(0)|. \end{aligned} \tag{26}$$

In the analysis of the dynamics of the coupled system it is very instructive to assume that at time $t = 0$ its quantum state is uncorrelated, i.e., it is described for a pure state obtained as a direct product

$$|\varphi(0)\rangle = |\beta\rangle \otimes |\psi_x\rangle \otimes |\psi_y\rangle, \tag{27}$$

where $|\psi_{x,y}\rangle$ are the coupling potential initial states. In spite of their apparent simplicity two-level coupled systems usually exhibit in its dynamics a quite complicated behaviour and fully quantum-mechanical effects. Many details of the dynamics of the system strongly depend on its initial condition, and in order to understand the global influence of the shape-invariant potentials on the system dynamics, in this study, we consider at $t = 0$ that both potentials are in coherent states and the two-level atom is in the lower state $|\beta\rangle = |-\rangle$.

The nth excited state of the Hamiltonians $\hat{\mathcal{H}}_{\pm}^{(\alpha)}$ for shape-invariant systems satisfy the eigenvalue equations [9]

$$\hat{\mathcal{H}}_{-}^{(\alpha)}|n\rangle_{\alpha} = e_n^{(\alpha)}|n\rangle_{\alpha} \qquad \text{and} \qquad \hat{\mathcal{H}}_{+}^{(\alpha)}|n\rangle_{\alpha} = \left[e_n^{(\alpha)} + R_{\alpha}\left(a_0^{(\alpha)}\right)\right]|n\rangle_{\alpha}, \tag{28}$$

with the correspondents eigenvalues given by $e_0^{(\alpha)} = 0$ and

$$e_n^{(\alpha)} = \sum_{k=1}^{n} R_{\alpha}\left(a_k^{(\alpha)}\right), \qquad \text{for} \quad n \geqslant 1. \tag{29}$$

In a previous work [15], we showed that the coherent states for shape-invariant systems with an infinite number of the bound state energy levels can be obtained in a generalized way by the expansion in the basis $\{|n\rangle_{\alpha}; n = 1, 2, 3, \ldots\}$,

$$\begin{aligned} &\left|z; a_r^{(\alpha)}\right\rangle = \sum_{n=0}^{\infty} \frac{z^n}{h_n\left(a_r^{(\alpha)}\right)}|n\rangle_{\alpha} \qquad \text{with} \quad h_0\left(a_r^{(\alpha)}\right) = 1, \\ &h_n\left(a_r^{(\alpha)}\right) = \prod_{s=0}^{n-1}\left[\frac{\sqrt{e_n^{(\alpha)} - e_s^{(\alpha)}}}{\mathcal{Z}_{j+s}^{(\alpha)}}\right], \qquad \text{for} \quad n \geqslant 1. \end{aligned} \tag{30}$$

In this expression $\mathcal{Z}_{j+s}^{(\alpha)} = \hat{T}_{\alpha}^{s}\mathcal{Z}_j^{(\alpha)}\hat{T}_{\alpha}^{\dagger s} = \mathcal{Z}^{(\alpha)}\left(a_{1+s}^{(\alpha)}, a_{2+s}^{(\alpha)}, a_{3+s}^{(\alpha)}, \ldots\right)$, being $\mathcal{Z}_j^{(\alpha)} \equiv \mathcal{Z}^{(\alpha)}\left(a_1^{(\alpha)}, a_2^{(\alpha)}, a_3^{(\alpha)}, \ldots\right)$ an arbitrary functional of the potential parameters.

With these assumptions the initial state of the coupled system is described by

$$|\varphi(0)\rangle = |-\rangle \otimes |\psi_x\rangle \otimes |\psi_y\rangle = \sum_{n_x=0}^{\infty}\sum_{n_y=0}^{\infty} b_{n_x}^{(x)} b_{n_y}^{(y)} |n_x\rangle_x \otimes |n_y\rangle_y \otimes |-\rangle, \tag{31}$$

where, by equation (30), $b_{n_\alpha}^{(\alpha)} = z_\alpha^{n_\alpha} \big/ h_{n_\alpha}^{(\alpha)}\big(a_r^{(\alpha)}\big) \in \mathbb{C}$ with $\alpha = x$ or y.

For any analytical function $f(x)$ it is easy to show that

$$\hat{B}_\pm^{(\alpha)} f\big(\hat{B}_\mp^{(\alpha)}\hat{B}_\pm^{(\alpha)}\big) = f\big(\hat{B}_\pm^{(\alpha)}\hat{B}_\mp^{(\alpha)}\big)\hat{B}_\pm^{(\alpha)}. \tag{32}$$

Using this property and expression (31) to get $\hat{\rho}_{\rm o}$, it is possible to show that the time-evolved density operator (26) can be explicitly expressed in the matrix form

$$\hat{\boldsymbol{\rho}}_\xi^{(\rm X)}(t) = \frac{1}{\mathcal{N}}\begin{bmatrix} \big|\mathcal{D}_\xi^{(\rm X)}(t)\big\rangle\big\langle\mathcal{D}_\xi^{(\rm X)}(t)\big| & \big|\mathcal{D}_\xi^{(\rm X)}(t)\big\rangle\big\langle\mathcal{C}_\xi^{(\rm X)}(t)\big| \\ \big|\mathcal{C}_\xi^{(\rm X)}(t)\big\rangle\big\langle\mathcal{D}_\xi^{(\rm X)}(t)\big| & \big|\mathcal{C}_\xi^{(\rm X)}(t)\big\rangle\big\langle\mathcal{C}_\xi^{(\rm X)}(t)\big| \end{bmatrix}, \tag{33}$$

where the factor

$$\mathcal{N} = \langle\varphi(0)|\varphi(0)\rangle = \sum_{n_x=0}^{\infty}\sum_{n_y=0}^{\infty} \big|b_{n_x}^{(x)}\big|^2\big|b_{n_y}^{(y)}\big|^2 \tag{34}$$

was introduced to have the normalization condition $\mathrm{Tr}\big(\hat{\rho}_\xi^{(\rm X)}(t)\big) = 1$ satisfied. The time-dependent states which compose the elements of the matrix $\hat{\boldsymbol{\rho}}_\xi^{(\rm X)}$ are expressed by

$$\big|\mathcal{C}_\xi^{(\rm X)}(t)\big\rangle = \exp\big(-\mathrm{i}\hat{\mathcal{H}}_{xy}^{(\rm X)}\Omega t\big)\cos\big(g\hat{\mu}_\xi^{(\rm X)}t\big)|\psi_{x,y}\rangle \tag{35}$$

$$\big|\mathcal{D}_\xi^{(\rm X)}(t)\big\rangle = \mathrm{i}\hat{F}_\xi^{(\rm X)}\exp\big(-\mathrm{i}\hat{\mathcal{H}}_{xy}^{(\rm X)}\Omega t\big)\sin\big(g\hat{\mu}_\xi^{(\rm X)}t\big)|\psi_{x,y}\rangle, \tag{36}$$

with

$$\hat{\mathcal{H}}_{xy}^{(\rm D)} = \hat{\mathcal{H}}_-^{(x)} + \hat{\mathcal{H}}_-^{(y)}, \qquad \hat{\mathcal{H}}_{xy}^{(\rm C)} = \hat{\mathcal{H}}_-^{(x)} + \hat{\mathcal{H}}_+^{(y)} \qquad \text{and} \qquad |\psi_{x,y}\rangle = |\psi_x\rangle \otimes |\psi_y\rangle. \tag{37}$$

In order to explore the dynamics of each subsystem which compose the coupled system we need to calculate from the density operator $\hat{\rho}_\xi^{(\rm X)}(t)$ the reduced density operator for either the atom or the coupling potentials. Tracing out the coupling potentials $V_x^{(\pm)}(x)$ and $V_y^{(\pm)}(y)$ degrees of freedom $\hat{\rho}_{\rm A}^{(\rm X,\xi)}(t) = \mathrm{Tr}_{1,2}\big\{\hat{\rho}_\xi^{(\rm X)}(t)\big\}$, we obtain the atom reduced 2×2 density matrix $\hat{\boldsymbol{\rho}}_{\rm A}^{(\rm X,\xi)}(t)$ whose elements are given by

$$\big\{\hat{\boldsymbol{\rho}}_{\rm A}^{(\rm X,\xi)}(t)\big\}_{jk} = \sum_{n_x=0}^{\infty}\sum_{n_y=0}^{\infty}\langle n_x, n_y|\big\{\hat{\boldsymbol{\rho}}_\xi^{(\rm X)}(t)\big\}_{jk}|n_x, n_y\rangle, \tag{38}$$

with $|n_x, n_y\rangle = |n_x\rangle \otimes |n_y\rangle$. In the same way the coupling potentials reduced density operator, obtained from $\hat{\rho}_{\rm P}^{(\rm X,\xi)}(t) = \mathrm{Tr}_{\rm A}\big\{\hat{\rho}_\xi^{(\rm X)}(t)\big\}$, gives

$$\begin{aligned}\hat{\rho}_{\rm P}^{(\rm X,\xi)}(t) &= \big\{\hat{\boldsymbol{\rho}}_\xi^{(\rm X)}(t)\big\}_{11} + \big\{\hat{\boldsymbol{\rho}}_\xi^{(\rm X)}(t)\big\}_{22} \\ &= \frac{1}{\mathcal{N}}\big(\big|\mathcal{C}_\xi^{(\rm X)}(t)\big\rangle\big\langle\mathcal{C}_\xi^{(\rm X)}(t)\big| + \big|\mathcal{D}_\xi^{(\rm X)}(t)\big\rangle\big\langle\mathcal{D}_\xi^{(\rm X)}(t)\big|\big).\end{aligned} \tag{39}$$

3. Temporal behaviour of the quantum dynamical variables

3.1. Population inversion factor

For a coupled two-level system the population inversion factor, also called the degree of excitation of the system [17, 18], and defined as $\hat{\rm W} \equiv \hat{\sigma}_+\hat{\sigma}_- - \hat{\sigma}_-\hat{\sigma}_+ = \hat{\sigma}_3$, is the simplest

nontrivial physical quantity to be used to analyse its quantum dynamic behaviour. In this case, inserting the time-evolved density operator (26) into equation (25) and taking into account the commutation property between $\hat{h}_0^{(\mathrm{X})}$ and $\hat{\mathcal{T}}_{\mathrm{X}}$ with $\hat{\sigma}_3$, we obtain the expectation value

$$\left\langle \hat{\mathrm{W}}_{\xi}^{(\mathrm{X})}(t) \right\rangle = \frac{\langle \varphi(0)|\hat{\rho}_{\mathrm{o}} \hat{U}_{\xi}^{(\mathrm{X})\dagger}(t,0)\hat{\sigma}_3 \hat{U}_{\xi}^{(\mathrm{X})}(t,0)|\varphi(0)\rangle}{\langle \varphi(0)|\hat{\rho}_{\mathrm{o}}|\varphi(0)\rangle}. \tag{40}$$

For both models, by using property (32) and equation (19) for $\hat{U}_{\xi}^{(\mathrm{X})}(t,0)$ in (40), we can show that

$$\left\langle \hat{\mathrm{W}}_{\xi}^{(\mathrm{X})}(t) \right\rangle = \frac{1}{\langle \varphi(0)|\varphi(0)\rangle} \left\{ \langle \varphi(0)| \begin{bmatrix} \cos\left(2g\hat{\omega}_{\xi}^{(\mathrm{X})}t\right) & \mathrm{i}\left\{\sin\left(2g\hat{\omega}_{\xi}^{(\mathrm{X})}t\right)\right\}\hat{F}_{\xi}^{(\mathrm{X})} \\ -\mathrm{i}\left\{\sin\left(2g\hat{\mu}_{\xi}^{(\mathrm{X})}t\right)\right\}\hat{G}_{\xi}^{(\mathrm{X})} & -\cos\left(2g\hat{\mu}_{\xi}^{(\mathrm{X})}t\right) \end{bmatrix} |\varphi(0)\rangle \right\}. \tag{41}$$

When we consider the initial state of system (31) in (41) we find the general expression

$$\left\langle \hat{\mathrm{W}}_{\xi}^{(\mathrm{X})}(t) \right\rangle = -\sum_{n_x,n_x'=0}^{\infty} b_{n_x}^{(x)*} b_{n_x'}^{(x)} \sum_{n_y,n_y'=0}^{\infty} b_{n_y}^{(y)*} b_{n_y'}^{(y)} \langle n_x, n_y|\cos\left(2g\hat{\mu}_{\xi}^{(\mathrm{X})}t\right)|n_x', n_y'\rangle \Big/ \sum_{n_x,n_y=0}^{\infty} \left|b_{n_x}^{(x)}\right|^2 \left|b_{n_y}^{(y)}\right|^2, \tag{42}$$

which, using the series expansion of the cosine function, the expressions (28), (20), (21) and the commutation between any function of $a_n^{(\alpha)}$ and the operators $\hat{\mathcal{T}}_{\pm}^{(\alpha)}$, can be written in the final form

$$\left\langle \hat{\mathrm{W}}_{\xi}^{(\mathrm{X})}(t) \right\rangle = -\sum_{n_x=0}^{\infty} \sum_{n_y=0}^{\infty} P_{n_x n_y} \cos\left(2g\vartheta_{n_x n_y}^{(\mathrm{X},\xi)}t\right), \tag{43}$$

where the weight is given by

$$P_{n_x n_y} = p_{n_x}^{(x)} p_{n_y}^{(y)} \Big/ \sum_{n_x,n_y=0}^{\infty} p_{n_x}^{(x)} p_{n_y}^{(y)} \qquad \text{with} \qquad p_n^{(\alpha)} = \left|b_n^{(\alpha)}\right|^2, \qquad \alpha = x \text{ or } y, \tag{44}$$

while the function argument factors have the forms

$$\sqrt{\vartheta_{n_x n_y}^{(\mathrm{D,N})}} = \vartheta_{n_x n_y}^{(\mathrm{D,U})} = \sqrt{e_{n_x}^{(x)} e_{n_y}^{(y)}} \qquad \text{and} \qquad \sqrt{\vartheta_{n_x n_y}^{(\mathrm{C,N})}} = \vartheta_{n_x n_y}^{(\mathrm{C,U})} = \sqrt{e_{n_x}^{(x)}\left[e_{n_y}^{(y)} + R_y\left(a_0^{(y)}\right)\right]}. \tag{45}$$

To conclude this section we observe that the dynamics of $\left\langle \hat{\mathrm{W}}_{\xi}^{(\mathrm{X})}(t) \right\rangle$, given by relation (43), is obtained with the sum of contributions from which the time-independent weight $P_{n_x n_y}$ is determined by the coupling potentials' initial state. The influence in these contributions of the kind of interaction characteristic of each model studied appears only in the argument factors $\vartheta_{n_x n_y}^{(\mathrm{X},\xi)}$ of the time-dependent circular function.

3.2. Entropy and entanglement of the system

Because of its simplicity and analyticity coupled models based on the dipole and rotating wave approximations offer an excellent laboratory to investigate the entanglement effects among different subsystems and its dynamical behaviour. Quantum entanglement has attracted much attention in recent years due to its potential applications in quantum communications, information processing and quantum computation. On the other hand, it has been shown [20, 21] that entropy is a very useful operational tool to quantify the entanglement of a given

system since, unlike other observables, the entropy is sensitive to all moments of the density operator.

Quantum mechanically the entropy is defined in terms of the density operator as [22] $S = -\mathrm{Tr}\{\hat{\rho}\ln\hat{\rho}\}$ when setting Boltzmann's constant $k_{\mathrm{B}} = 1$. If $\hat{\rho}$ describes a pure state this entropy vanishes ($S = 0$), while if $\hat{\rho}$ describes a mixed state then $S \neq 0$. Therefore, entropy offers a quantitative measure of the disorder of a system, and of the purity of a quantum state. The higher the entropy, the greater the entanglement of the system. The trace of an operator depends only on its eigenvalues; then since $\hat{\rho}$ is governed by a unitary time evolution and consequently its eigenvalues remain constant, the same is true for any function of $\hat{\rho}$ which imply that the entropy S is constant, as expected for a closed system. Of more interest, therefore, are the partial entropies of system components, such as the atom and the coupling potentials subsystems in our study. These partial entropies, when treated as separate system, are defined through the corresponding reduced density operators by

$$\begin{aligned} S_{\mathrm{A}}^{(\mathrm{X},\xi)}(t) &= -\mathrm{Tr}_{\mathrm{A}}\left\{\hat{\rho}_{\mathrm{A}}^{(\mathrm{X},\xi)}(t)\ln\left[\hat{\rho}_{\mathrm{A}}^{(\mathrm{X},\xi)}(t)\right]\right\} \qquad \text{and} \\ S_{\mathrm{P}}^{(\mathrm{X},\xi)}(t) &= -\mathrm{Tr}_{\mathrm{P}}\left\{\hat{\rho}_{\mathrm{P}}^{(\mathrm{X},\xi)}(t)\ln\left[\hat{\rho}_{\mathrm{P}}^{(\mathrm{X},\xi)}(t)\right]\right\}. \end{aligned} \tag{46}$$

Note that the operation of tracing over part of the whole systems' variables means that $\hat{\rho}_{\mathrm{A(P)}}^{(\mathrm{X},\xi)}(t)$ is no longer governed by a unitary time evolution and consequently $S_{\mathrm{A(P)}}^{(\mathrm{X},\xi)}(t)$ is no longer time independent. This implies that a subsystem can evolve from a pure to a mixed state and vice versa with oscillations in the subsystem entropy.

Taken as a whole, the two-level atom coupled to a two-dimensional shape-invariant system in an overall pure state constitutes a tripartite quantum system in a Hilbert space with a tensor product structure $\mathcal{E} = \mathcal{E}_x \otimes \mathcal{E}_y \otimes \mathcal{E}_{\mathrm{A}}$. However, in our study we work with the entire coupling potentials Hilbert subspace $\mathcal{E}_{xy} = \mathcal{E}_x \otimes \mathcal{E}_y$. With this procedure we reduce our study to a correspondent bipartite quantum system in a Hilbert space $\mathcal{E} = \mathcal{E}_{xy} \otimes \mathcal{E}_{\mathrm{A}}$. In these conditions the Araki and Lieb theorem [23] is valid and if the combined system begins as a pure quantum state (that is, the total entropy of the system is equal to zero), then at $t > 0$ the partial entropies of the subsystems are precisely equal. Under these circumstances, if we consider that trace is invariant in a similarity transformation, we can go to a basis in which $\hat{\rho}_{\mathrm{P}}^{(\mathrm{X},\xi)}(t)$ is diagonal to evaluate the coupling potentials partial entropy with the expression

$$S_{\mathrm{P}}^{(\mathrm{X},\xi)}(t) = -\left\{\lambda_{\mathrm{P}}^{(\mathrm{X},\xi,-)}(t)\ln\left[\lambda_{\mathrm{P}}^{(\mathrm{X},\xi,-)}(t)\right] + \lambda_{\mathrm{P}}^{(\mathrm{X},\xi,+)}(t)\ln\left[\lambda_{\mathrm{P}}^{(\mathrm{X},\xi,+)}(t)\right]\right\} \tag{47}$$

obtained from equation (46), where $\lambda_{\mathrm{P}}^{(\mathrm{X},\xi,\pm)}(t)$ are the eigenvalues of $\hat{\rho}_{\mathrm{P}}^{(\mathrm{X},\xi)}(t)$.

Considering the eigenvalue equation $\hat{\rho}_{\mathrm{P}}^{(\mathrm{X},\xi)}\left|\zeta_{\mathrm{P}}^{(\mathrm{X},\xi)}\right\rangle = \lambda_{\mathrm{P}}^{(\mathrm{X},\xi,\pm)}\left|\zeta_{\mathrm{P}}^{(\mathrm{X},\xi)}\right\rangle$ and looking at expression (39) of $\hat{\rho}_{\mathrm{P}}^{(\mathrm{X},\xi)}(t)$, we expect that its eigenstates have the form $\left|\zeta_{\mathrm{P}}^{(\mathrm{X},\xi)}(t)\right\rangle = \Lambda_{\mathcal{C}}(t)\left|\mathcal{C}_{\xi}^{(\mathrm{X})}(t)\right\rangle + \Lambda_{\mathcal{D}}(t)\left|\mathcal{D}_{\xi}^{(\mathrm{X})}(t)\right\rangle$ so that

$$\begin{aligned} \hat{\rho}_{\mathrm{P}}^{(\mathrm{X},\xi)}(t)\left|\zeta_{\mathrm{P}}^{(\mathrm{X},\xi)}(t)\right\rangle = {} & \frac{1}{\mathcal{N}}\left(\left\langle\mathcal{C}_{\xi}^{(\mathrm{X})}(t)\middle|\mathcal{C}_{\xi}^{(\mathrm{X})}(t)\right\rangle + \frac{\Lambda_{\mathcal{D}}(t)}{\Lambda_{\mathcal{C}}(t)}\left\langle\mathcal{C}_{\xi}^{(\mathrm{X})}(t)\middle|\mathcal{D}_{\xi}^{(\mathrm{X})}(t)\right\rangle\right)\Lambda_{\mathcal{C}}(t)\left|\mathcal{C}_{\xi}^{(\mathrm{X})}(t)\right\rangle \\ & + \frac{1}{\mathcal{N}}\left(\left\langle\mathcal{D}_{\xi}^{(\mathrm{X})}(t)\middle|\mathcal{D}_{\xi}^{(\mathrm{X})}(t)\right\rangle + \frac{\Lambda_{\mathcal{C}}(t)}{\Lambda_{\mathcal{D}}(t)}\left\langle\mathcal{D}_{\xi}^{(\mathrm{X})}(t)\middle|\mathcal{C}_{\xi}^{(\mathrm{X})}(t)\right\rangle\right)\Lambda_{\mathcal{D}}(t)\left|\mathcal{D}_{\xi}^{(\mathrm{X})}(t)\right\rangle \end{aligned} \tag{48}$$

and, consequently, for $\left|\zeta_{\mathrm{P}}^{(\mathrm{X},\xi)}(t)\right\rangle$ to be an eigenstate of $\hat{\rho}_{\mathrm{P}}^{(\mathrm{X},\xi)}(t)$, we must have satisfied the condition

$$\begin{aligned} \mathcal{N}\lambda_{\mathrm{P}}^{(\mathrm{X},\xi,\pm)}(t) &= \left\langle\mathcal{C}_{\xi}^{(\mathrm{X})}(t)\middle|\mathcal{C}_{\xi}^{(\mathrm{X})}(t)\right\rangle + \frac{\Lambda_{\mathcal{D}}(t)}{\Lambda_{\mathcal{C}}(t)}\left\langle\mathcal{C}_{\xi}^{(\mathrm{X})}(t)\middle|\mathcal{D}_{\xi}^{(\mathrm{X})}(t)\right\rangle \\ &= \left\langle\mathcal{D}_{\xi}^{(\mathrm{X})}(t)\middle|\mathcal{D}_{\xi}^{(\mathrm{X})}(t)\right\rangle + \frac{\Lambda_{\mathcal{C}}(t)}{\Lambda_{\mathcal{D}}(t)}\left\langle\mathcal{D}_{\xi}^{(\mathrm{X})}(t)\middle|\mathcal{C}_{\xi}^{(\mathrm{X})}(t)\right\rangle. \end{aligned} \tag{49}$$

In this point if we consider that in general $\langle \mathcal{C}_\xi^{(\mathrm{X})}(t)|\mathcal{C}_\xi^{(\mathrm{X})}(t)\rangle, \langle \mathcal{D}_\xi^{(\mathrm{X})}(t)|\mathcal{D}_\xi^{(\mathrm{X})}(t)\rangle \neq 1$ and $\langle \mathcal{C}_\xi^{(\mathrm{X})}(t)|\mathcal{D}_\xi^{(\mathrm{X})}(t)\rangle \neq 0$ and take into account that $\langle \mathcal{C}_\xi^{(\mathrm{X})}(t)|\mathcal{C}_\xi^{(\mathrm{X})}(t)\rangle + \langle \mathcal{D}_\xi^{(\mathrm{X})}(t)|\mathcal{D}_\xi^{(\mathrm{X})}(t)\rangle = \mathcal{N}$, we can show, after some calculations, that

$$\lambda_{\mathrm{P}}^{(\mathrm{X},\xi,\pm)}(t) = \frac{1}{2}\left(1 \pm \frac{1}{\mathcal{N}}\sqrt{\left[\langle \mathcal{C}_\xi^{(\mathrm{X})}(t)|\mathcal{C}_\xi^{(\mathrm{X})}(t)\rangle - \langle \mathcal{D}_\xi^{(\mathrm{X})}(t)|\mathcal{D}_\xi^{(\mathrm{X})}(t)\rangle\right]^2 + 4\left|\langle \mathcal{C}_\xi^{(\mathrm{X})}(t)|\mathcal{D}_\xi^{(\mathrm{X})}(t)\rangle\right|^2}\right). \tag{50}$$

As shown in [11], $\hat{B}_+^{(\alpha)}|n\rangle_\alpha = \sqrt{e_{n+1}^{(\alpha)}}|n+1\rangle_\alpha$ and $\hat{B}_-^{(\alpha)}|n\rangle_\alpha = \sqrt{e_{n-1}^{(\alpha)} + R_\alpha\left(a_0^{(\alpha)}\right)}|n-1\rangle_\alpha$. These results permit us to evaluate the action of the operator $\hat{F}_\xi^{(\mathrm{X})}$ on $|n\rangle_\alpha$ that together with relations (36), (37) and the action of the operators $\hat{\mathcal{H}}_\pm^{(\alpha)}$ and $\hat{\mu}_\xi^{(\mathrm{X})}$ on the same states gives the final expressions for the factors that appear in (50)

$$\frac{1}{\mathcal{N}}\langle \mathcal{C}_\xi^{(\mathrm{X})}(t)|\mathcal{C}_\xi^{(\mathrm{X})}(t)\rangle = \sum_{n_x=0}^{\infty}\sum_{n_y=0}^{\infty} P_{n_x n_y}\cos^2\left(g\vartheta_{n_x n_y}^{(\mathrm{X},\xi)}t\right) \tag{51}$$

$$\frac{1}{\mathcal{N}}\langle \mathcal{D}_\xi^{(\mathrm{X})}(t)|\mathcal{D}_\xi^{(\mathrm{X})}(t)\rangle = \sum_{n_x=0}^{\infty}\sum_{n_y=0}^{\infty} P_{n_x n_y}\sin^2\left(g\vartheta_{n_x n_y}^{(\mathrm{X},\xi)}t\right), \tag{52}$$

where the weight $P_{n_x n_y}$ and the argument factors $\vartheta_{n_x n_y}^{(\mathrm{X},\xi)}$ are given by (44) and (45), respectively. On the other hand, using expression (30) and the definition of the $b_n^{(\alpha)}$ expansion coefficients it is possible to establish the relations

$$\hat{T}_\alpha^\dagger b_{n+1}^{(\alpha)}\hat{T}_\alpha = \frac{z_\alpha \mathcal{Z}_{j_\alpha-1}^{(\alpha)}}{\sqrt{e_n^{(\alpha)} + R_\alpha\left(a_0^{(\alpha)}\right)}}b_n^{(\alpha)} \qquad \text{and} \qquad \hat{T}_\alpha b_{n-1}^{(\alpha)}\hat{T}_\alpha^\dagger = \frac{\sqrt{e_n^{(\alpha)}}}{z_\alpha \mathcal{Z}_{j_\alpha}^{(\alpha)}}b_n^{(\alpha)} \tag{53}$$

and, with the help of these relations, to show that

$$\frac{1}{\mathcal{N}}\left|\langle \mathcal{C}_\xi^{(\mathrm{X})}(t)|\mathcal{D}_\xi^{(\mathrm{X})}(t)\rangle\right| = \left|\sum_{n_x=0}^{\infty}\sum_{n_y=0}^{\infty}\Theta_{n_x n_y}^{(\mathrm{X})}P_{n_x n_y}\cos\left(g\vartheta_{n_x n_y}^{(\mathrm{X},\xi)}t\right)\sin\left(g\Upsilon_{n_x n_y}^{(\mathrm{X},\xi)}t\right)\right|, \tag{54}$$

where

$$\begin{aligned}\Theta_{n_x n_y}^{(\mathrm{D})} &= \frac{\left|z_x z_y \mathcal{Z}_{j_x-1}^{(x)}\mathcal{Z}_{j_y-1}^{(y)}\right|}{\sqrt{\left[e_{n_x}^{(x)} + R_x\left(a_0^{(x)}\right)\right]\left[e_{n_y}^{(y)} + R_y\left(a_0^{(y)}\right)\right]}},\\ \Theta_{n_x n_y}^{(\mathrm{C})} &= \left|\frac{z_x \mathcal{Z}_{j_x-1}^{(x)}}{z_y \mathcal{Z}_{j_y}^{(y)}}\right|\sqrt{\frac{e_{n_y}^{(y)}}{e_{n_x}^{(x)} + R_x\left(a_0^{(x)}\right)}};\end{aligned} \tag{55}$$

$$\begin{aligned}\sqrt{\Upsilon_{n_x n_y}^{(\mathrm{D,N})}} &= \Upsilon_{n_x n_y}^{(\mathrm{D,U})} = \sqrt{\left[e_{n_x}^{(x)} + R_x\left(a_0^{(x)}\right)\right]\left[e_{n_y}^{(y)} + R_y\left(a_0^{(y)}\right)\right]},\\ \sqrt{\Upsilon_{n_x n_y}^{(\mathrm{C,N})}} &= \Upsilon_{n_x n_y}^{(\mathrm{C,U})} = \sqrt{\left[e_{n_x}^{(x)} + R_x\left(a_0^{(x)}\right)\right]e_{n_y}^{(y)}}.\end{aligned} \tag{56}$$

Finally, it is worth noting that the atomic partial entropy can be obtained from the expression $S_{\mathrm{A}}^{(\mathrm{X},\xi)}(t) = -\left\{\lambda_{\mathrm{A}}^{(\mathrm{X},\xi,-)}(t)\ln\left[\lambda_{\mathrm{A}}^{(\mathrm{X},\xi,-)}(t)\right] + \lambda_{\mathrm{A}}^{(\mathrm{X},\xi,+)}(t)\ln\left[\lambda_{\mathrm{A}}^{(\mathrm{X},\xi,+)}(t)\right]\right\}$, where $\lambda_{\mathrm{A}}^{(\mathrm{X},\xi,\pm)}(t)$ are the eigenvalues of $\hat{\rho}_{\mathrm{A}}^{(\mathrm{X},\xi)}(t)$. These eigenvalues are determined by applying the

diagonalization procedure with the solution of the secular equation $\left|\hat{\boldsymbol{\rho}}_{\mathrm{A}}^{(\mathrm{X},\xi)} - \lambda_{\mathrm{A}}^{(\mathrm{X},\xi,\pm)}\hat{\mathbf{1}}\right| = 0$ whose roots are given by

$$\lambda_{\mathrm{A}}^{(\mathrm{X},\xi,\pm)}(t) = \frac{1}{2}\left(1 \pm \sqrt{\left[\left\{\hat{\boldsymbol{\rho}}_{\mathrm{A}}^{(\mathrm{X},\xi)}(t)\right\}_{11} - \left\{\hat{\boldsymbol{\rho}}_{\mathrm{A}}^{(\mathrm{X},\xi)}(t)\right\}_{22}\right]^2 + 4\left|\left\{\hat{\boldsymbol{\rho}}_{\mathrm{A}}^{(\mathrm{X},\xi)}(t)\right\}_{12}\right|^2}\right). \tag{57}$$

Using the expression of the density matrix elements (38) and the completeness relation $\sum_{n_\alpha=0}^{\infty} |n_\alpha\rangle_{\alpha\alpha}\langle n_\alpha| = \hat{1}$, it is straightforward to show that (50) and (57) give the same result and thus $S_{\mathrm{P}}^{(\mathrm{X},\xi)}(t) = S_{\mathrm{A}}^{(\mathrm{X},\xi)}(t)$, as expected from the theorem of Araki and Lieb [23].

4. Applications for some pairs of shape-invariant potentials

In order to investigate how our general results can be applied in specific cases, we consider in this section the coupling of the two-level atom with three examples of pairs of shape-invariant potentials. The first one with two harmonic oscillator potentials, the second one with a harmonic oscillator and a Pösch–Teller potential, and the last one with a harmonic oscillator and a self-similar potential. Applying the general approach for a given pair of shape-invariant coupling potentials we need to specify only the energy spectra $e_{n_x}^{(x)}$ and $e_{n_y}^{(y)}$ as well the expansion coefficients $b_{n_x}^{(x)}$ and $b_{n_y}^{(y)}$ related with the initial state of the system. Using this information we obtain the function argument factors $\vartheta_{n_x n_y}^{(\mathrm{X},\xi)}$ and $\Upsilon_{n_x n_y}^{(\mathrm{X},\xi)}$, the weight $P_{n_x n_y}$ and the factors $\Theta_{n_x n_y}^{(\mathrm{X})}$. The numerical convergence of infinite series is a nontrivial problem, and thus we used the Smith package of Fortran subroutines [24] which performs floating-point multiple-precision arithmetic and elementary functions. Using this package we obtain a greater speed and higher precision in the calculations.

4.1. Coupling with two harmonic oscillator potentials (HO + HO)

We start with this example because the harmonic oscillator (HO) is the simplest among the shape-invariant coupling potentials. We would also like to show that, in some cases, our general expressions reduce to the well-known expressions previously obtained in studies involving matter–radiation interaction with two-photon processes. In this sense, the results obtained with this first application can be used as a reference for the following applications involving more complicated shape-invariant potentials.

The partner potentials (3) for these systems are obtained with the superpotentials $W\left(\alpha, a_1^{(\alpha)}\right) = \sqrt{\hbar\Omega}\left(a_1^{(\alpha)}\alpha + \delta_\alpha\right)$ with $\alpha = x$ or y, where $a_1^{(\alpha)}$ and δ_α are real constants, and $R_\alpha\left(a_n^{(\alpha)}\right) = \eta\left[a_n^{(\alpha)} + a_{n+1}^{(\alpha)}\right]$, $\eta = \sqrt{\hbar/(2M\Omega)}$. Since for these potentials $a_1^{(\alpha)} = a_2^{(\alpha)} = \cdots = a_n^{(\alpha)}$ we get $R_\alpha\left(a_n^{(\alpha)}\right) = \gamma_\alpha$, with $\gamma_\alpha = 2\eta a_1^{(\alpha)}$, and thus $e_{n_\alpha}^{(\alpha)} = n_\alpha\gamma_\alpha$. The constant values of the parameters $a_n^{(\alpha)}$ imply that for these systems we must have $\mathcal{Z}_{j_\alpha}^{(\alpha)} = c_\alpha$, a constant. Under these conditions equation (30) gives us $h_{n_\alpha}^{(\alpha)}\left(a_r^{(\alpha)}\right) = \sqrt{\gamma_\alpha^{n_\alpha} n_\alpha!}\big/c_\alpha^{n_\alpha}$. Redefining $z_\alpha \to c_\alpha z_\alpha/\sqrt{\gamma_\alpha}$, we find for the partial weight (44) and the coherent state (30)

$$p_{n_\alpha}^{(\alpha)} = \frac{|z_\alpha|^{2n_\alpha}}{n_\alpha!}, \qquad |z_\alpha; a_r\rangle_\alpha = \sum_{n_\alpha=0}^{\infty} \frac{z_\alpha^{n_\alpha}}{\sqrt{n_\alpha!}}|n_\alpha\rangle_\alpha, \qquad \alpha = x \text{ or } y, \tag{58}$$

which is the usual expression for bosonic coherent states [25]. Thus the function arguments (45) and (56), and factors (55) can be determined, and the results are shown in column HO + HO of table 1 presented below. Specified the expressions of these factors we get the population

Table 1. Factors and function arguments for each coupling potential system.

System	HO + HO	HO + PT	HO + SS
$\vartheta_{n_x n_y}^{(\mathrm{D,N})}$	$\gamma_{xy} n_x n_y$	$\gamma_{xy} n_x n_y (n_y + \nu_y + 1)$	$\frac{\gamma_{xy} n_x (1-q^{n_y})}{1-q}$
$\vartheta_{n_x n_y}^{(\mathrm{C,N})}$	$\gamma_{xy} n_x (n_y + 1)$	$\gamma_{xy} n_x [n_y (n_y + \nu_y + 1) + \nu_y]$	$\frac{\gamma_{xy} n_x (1-q^{n_y+1})}{q(1-q)}$
$\Upsilon_{n_x n_y}^{(\mathrm{D,N})}$	$\gamma_{xy} (n_x + 1)(n_y + 1)$	$\gamma_{xy} (n_x + 1)[n_y (n_y + \nu_y + 1) + \nu_y]$	$\frac{\gamma_{xy} (n_x+1)(1-q^{n_y+1})}{q(1-q)}$
$\Upsilon_{n_x n_y}^{(\mathrm{C,N})}$	$\gamma_{xy} (n_x + 1) n_y$	$\gamma_{xy} (n_x + 1) n_y (n_y + \nu_y + 1)$	$\frac{\gamma_{xy} (n_x+1)(1-q^{n_y})}{1-q}$
$\Theta_{n_x n_y}^{(\mathrm{D})}$	$\frac{\lvert z_x z_y \rvert}{\sqrt{(n_x+1)(n_y+1)}}$	$\frac{\lvert z_x z_y \rvert \sqrt{\nu_y(\nu_y-1)}}{\sqrt{(n_x+1)[n_y(n_y+\nu_y+1)+\nu_y]}}$	$\frac{\lvert z_x z_y \rvert \sqrt{R_y(a_1^{(y)})(1-q)}}{\sqrt{q(n_x+1)(1-q^{n_y+1})}}$
$\Theta_{n_x n_y}^{(\mathrm{C})}$	$\left\lvert \frac{z_x}{z_y} \right\rvert \sqrt{\frac{n_y}{n_x+1}}$	$\left\lvert \frac{z_x}{z_y} \right\rvert \sqrt{\frac{n_y(n_y+\nu_y+1)}{(n_x+1)(\nu_y+1)(\nu_y+2)}}$	$\left\lvert \frac{z_x}{z_y} \right\rvert \sqrt{\frac{1-q^{n_y}}{R_y(a_1^{(y)})(1-q)(n_x+1)}}$
γ_{xy}	$\gamma_x \gamma_y$	$\gamma_x \kappa_y^2$	$\gamma_x R_y(a_1^{(y)})$

Observation: $\vartheta_{n_x n_y}^{(\mathrm{X,U})} = \sqrt{\vartheta_{n_x n_y}^{(\mathrm{X,N})}}$ and $\Upsilon_{n_x n_y}^{(\mathrm{X,U})} = \sqrt{\Upsilon_{n_x n_y}^{(\mathrm{X,N})}}$.

inversion factor (43) and the coupling potentials partial entropy (47). In this case the weight function (44) assumes the form

$$P_{n_x n_y}(z_x, z_y) = \frac{|z_x|^{2n_x} |z_y|^{2n_y}}{n_x! n_y!} \, \mathrm{e}^{-(|z_x|^2 + |z_y|^2)}, \tag{59}$$

which corresponds to a product of two independent Poisson distributions centred at $|z_x|^2$ and $|z_y|^2$ with widths $|z_x|$ and $|z_y|$, respectively. Note that if we use (59) and $\vartheta_{n_x n_y}^{(\mathrm{C,U})}$ in (43), we obtain the result of [26] for the population inversion factor of the two-level atom interacting with two quantized cavity fields.

The numerical results for this application were obtained using shape-invariant potential coherent states with $|z_x|^2 = |z_y|^2 = 20$ and energy factor $\gamma_{xy} = 1$. In figure 1(*a*), we have plotted the population inversion factor $\langle \hat{\mathrm{W}}_{\mathrm{U}}^{(\mathrm{D})}(t) \rangle$ in terms of the time variable $\tau_{\mathrm{W}} = 2gt/\pi$. A first view of this figure gives the impression of a non-periodic succession of revivals and collapses events. However, a more careful observation reveals that there is some periodicity in these events. All revivals events have in common the same pattern shown in the middle small figure below and can be grouped as α, β, γ and δ revival events. The first three kinds of revival events present a common period of $\tau_\alpha \approx 4\tau_{\mathrm{W}}$, while the last one has $\tau_\delta \approx 6\tau_{\mathrm{W}}$. Some groups ($\alpha$ and δ) show a gradual reduction in their amplitude with the repetition process while other groups (β and γ) present an increasing process in their amplitude. However, an extension of the figure for longer times shows that each group of revival events has its amplitude modulated with a Gaussian envelope pattern characteristic of an isolated harmonic oscillator potential. Eventually, elements of different groups of events overlap with each other giving rise to a more complicated pattern that makes harder to distinguish them.

To understand the time behaviour of $\langle \hat{\mathrm{W}}_{\mathrm{U}}^{(\mathrm{D})}(t) \rangle$, we observe that each term in the double sum (43) has a different frequency, and as the time increases they become uncorrelated and interfere destructively, causing a collapse $\left[\langle \hat{\mathrm{W}}_{\mathrm{U}}^{(\mathrm{D})}(t) \rangle \approx 0 \right]$. The discrete character of the double sum over the quantum states in the coherent states ensures that, after some finite time, all the oscillating terms come back almost in phase with each other, restoring the coherent oscillations and creating periodic revivals (periodic packets of finite $\langle \hat{\mathrm{W}}_{\mathrm{U}}^{(\mathrm{D})}(t) \rangle$ oscillations). However, as the frequencies are not necessarily integers and thus may be incommensurate, the re-phasing is not perfect and the revivals get broader and broader. In our system the

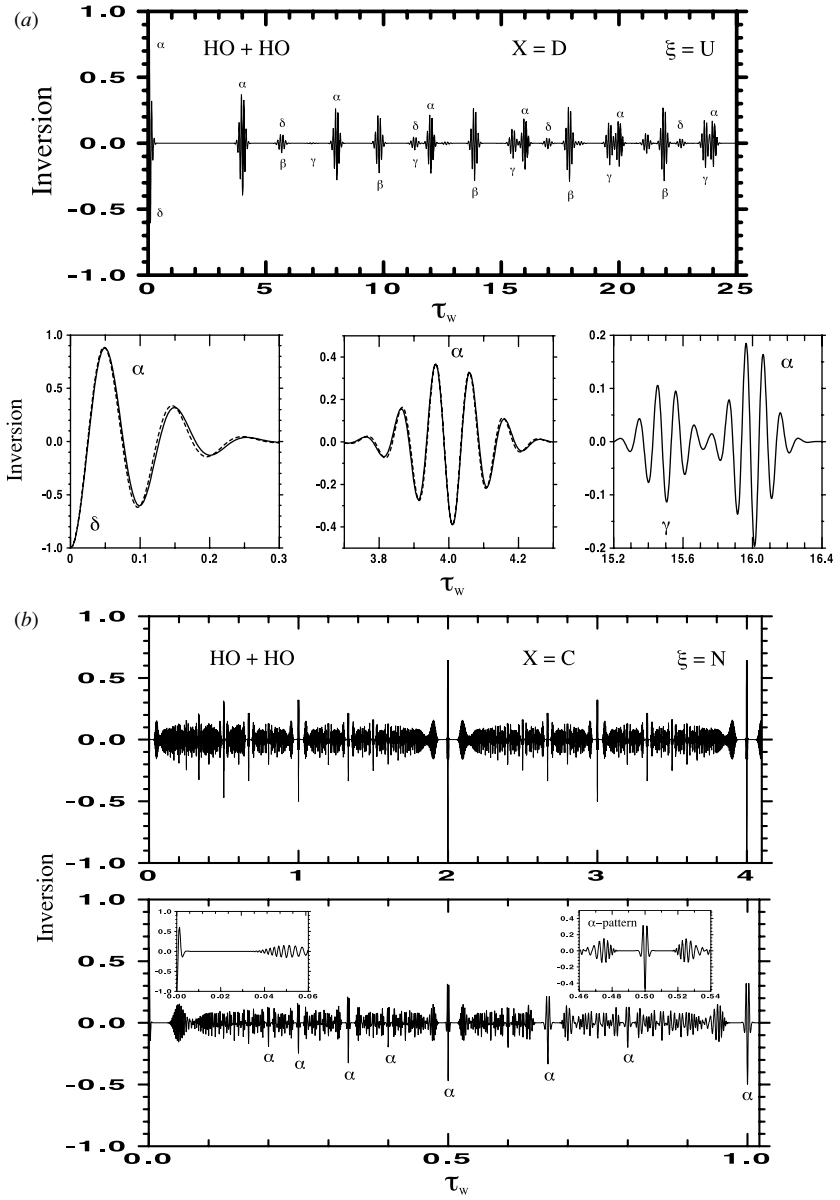

Figure 1. (*a*) Time evolution of the population inversion factor for two harmonic oscillator coupling potentials in the direct-coupled model and usual interaction case. The constant values used are $|z_x|^2 = |z_y|^2 = 20$ and $\gamma_{xy} = 1$. (*b*) Same as (*a*) for the conjugate-coupled model and intensity-dependent interaction calculated with the same strengths.

presence of two coupling potentials is responsible for the appearing of the double sum in the expression of $\langle \hat{W}_U^{(D)}(t) \rangle$ that opens a great number of the new re-phasing possibilities causing the appearing of new revival events. The periodic behaviour of the cosine function in time, the form of its argument and its dependence on the coupling potentials $e_{n_\alpha}^{(\alpha)}$ factors define the form and the periodicity of these events in $\langle \hat{W}_U^{(D)}(t) \rangle$.

In the bottom part of figure 1(*a*), we show the magnified views in time of the first collapse and some revival events in $\langle \hat{W}_U^{(D)}(t) \rangle$ (solid lines) together with the results obtained for the population inversion factor $\langle \hat{W}_U^{(C)}(t) \rangle$ (dashed lines). We conclude in this case that the conjugate-coupled model presents only a little compression in the Rabi oscillation period of each revival event, effect that makes itself smaller for longer times. Indeed this small difference between the results of the two models is an expected result since the modification introduced with the conjugate-coupled model in relation to the direct one is only the change of $n_y \to n_y + 1$ in the time-dependent cosine function argument.

Figure 1(*b*) is the version of figure 1(*a*) for $\langle \hat{W}_N^{(C)}(t) \rangle$. Looking at the top part of this figure it is possible to identify an almost symmetric time cell, shown in detail in the bottom part of the figure, that is repeated periodically in time. Moreover, in this time cell it is possible to recognize the α-pattern, shown in detail in the second inset of the bottom figure, that is repeated many times inside the cell. It is easy to verify that the α-pattern is the symmetrized reproduction of the first collapse event, shown in a magnified time view in the first inset of the bottom figure. The periodic reproduction in time of a given pattern with enhancement effects in the quantum behaviour of an observable is the characteristic property of the intensity-dependent interaction in the models based on the dipole and rotating wave approximations. The reason of this characteristic is the absence of the square root in the cosine function time argument. This fact makes the Rabi frequencies commensurable what reinforce the re-phasing process in $\langle \hat{W}_N^{(C)}(t) \rangle$.

In figure 2(*a*), we have plotted the coupling potentials partial entropy $S_P^{(D,U)}(t)$ in terms of the time variable $\tau_S = \tau_W/2 = gt/\pi$. As we see from the figure, when the interaction is turned on, the entropy increases rapidly from the initial zero value starting a sequence of Rabi oscillations with decreasing amplitudes until it assumes the maximum value $S_{max} \approx 0.693$. This maximum value is obtained when the square root factor in (50) goes to zero and $\lambda_P^{(X,\xi,+)}(t) \to \lambda_P^{(X,\xi,-)}(t) \to \frac{1}{2}$. In these conditions equation (47) gives the value $S_P^{(X,\xi)}(t) = \ln 2 \approx 0.693$. This result is still valid for the bipartite quantum system in general. The entropy, after assuming the maximum level, shows depression regions with Rabi oscillation packets temporally coincident with the arrival events in $\langle \hat{W}_U^{(D)}(t) \rangle$. Looking at the magnified view of the entropy oscillations in the bottom part of the figure and comparing with the revival events in the inversion population factor it is easy to recognize some resemblance in the pattern of the oscillations in both observables. Like $\langle \hat{W}_\xi^{(X)}(t) \rangle$, the partial entropy for the direct model (solid line) and conjugate-coupled model (dashed line) has almost similar time evolution.

In terms of the system entanglement, using the entropy behaviour we can say that the system starts in a pure quantum state, when the entropy is null and the coupling potentials are completely disentangled from the two-level atom, and evolves to a mixed quantum state, when the entropy assumes its maximum value S_{max}, and the coupling potentials are strongly entangled with the two-level atom. In the entropy oscillations and in its decreasing process the system roughly returns to pure quantum states, increasing the disentanglement of the coupled system.

Figure 2(*b*) is the conjugate-coupled model and intensity-dependent version of figure 2(*a*). Relevant aspects to learn in this case are (i) the perfect symmetry of the time cell of $S_P^{(C,N)}(t)$, which is shown in detail in the bottom part of the figure; (ii) the return of the system to the pure (completely disentangled) quantum initial state when $\tau = n\tau_S$ with $n \in \mathbb{Z}$. Thus we conclude that $S_P^{(X,\xi)}(t)$ shows more time symmetry and revival properties than $\langle \hat{W}_\xi^{(X)}(t) \rangle$. The α-pattern that is repeated many times in the time cell is shown in detail in the second inset of the bottom figure.

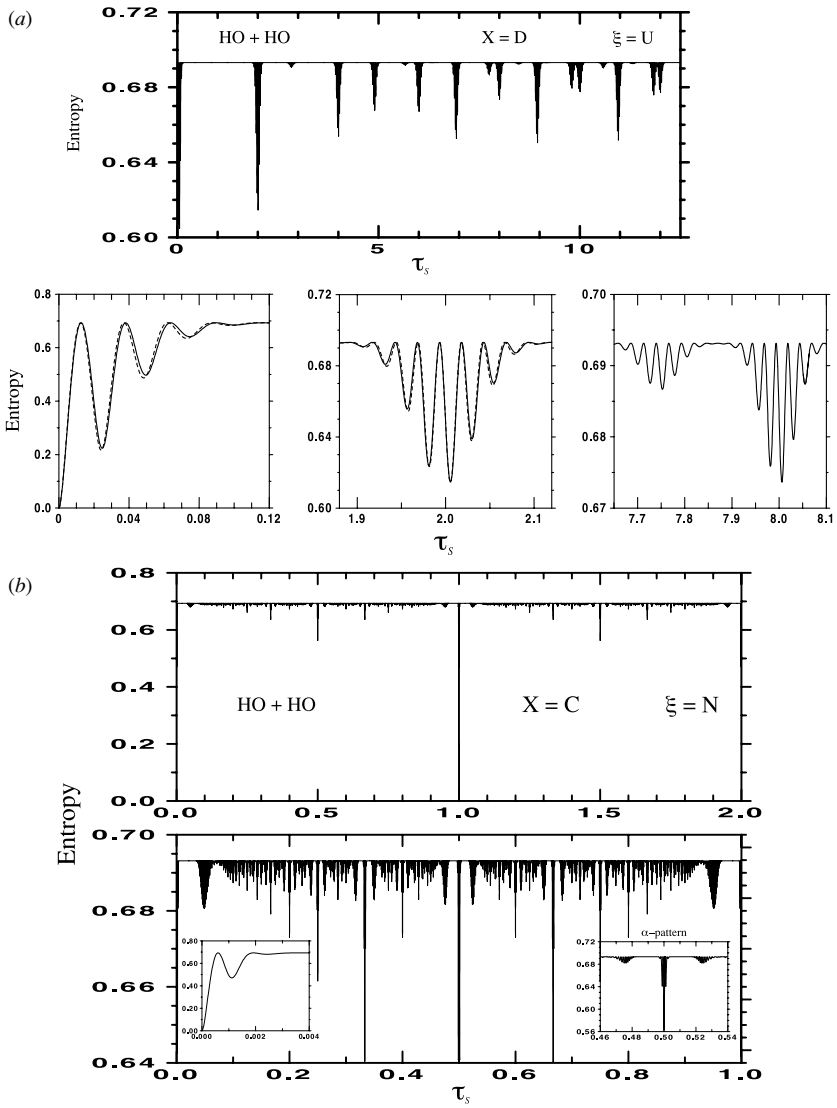

Figure 2. (*a*) Time evolution of the coupling potentials partial entropy for two harmonic oscillator coupling potentials in the direct-coupled model and usual interaction case. The constant values used are $|z_x|^2 = |z_y|^2 = 20$ and $\gamma_{xy} = 1$. (*b*) Same as (*a*) for the conjugate coupled model and intensity-dependent interaction calculated with the same strengths.

4.2. Coupling with a harmonic oscillator and a Pöschl–Teller potentials (HO + PT)

The Pöschl–Teller (PT) potential, originally introduced in a molecular physics context [27], is closely related to several other potentials, widely used in molecular and solid state physics and, in addition, becomes the infinite square well in a limiting case. The inclusion of the Pöschl–Teller potential in our study permits us to evaluate the anharmonic and dissociation effects in the two-potential coupled system, which are related with a more realistic physical situation. In this sense, we assume that the partner potentials (3) for these shape-invariant coupling potential systems are obtained with the superpotentials

$W_x\big(x, a_1^{(x)}\big)$ for a harmonic oscillator, while for the Pöschl–Teller case [18] we have $W_y\big(y, a_1^{(y)}\big) = \sqrt{\hbar\Omega}\big\{\varrho_y(a_1^{(y)} + \gamma_y)\cot[\varrho_y(y+\lambda_y)] + \delta_y \csc[\varrho_y(y+\lambda_y)]\big\}$, where $\varrho_y, \gamma_y, \delta_y$ and λ_y are real constants. In this second case the remainders [2] in condition (4) are given by $R_y\big(a_{n_y}^{(y)}\big) = \varrho_y^2\eta\big[2(a_{n_y}^{(y)} + \gamma_y) + \eta\big]$, with the potential parameters related by $a_{n_y+1}^{(y)} = a_{n_y}^{(y)} + \eta$, where $\eta = \sqrt{\hbar/(2M\Omega)}$. Inserting these results into (29) we can prove that $\mathrm{e}_{n_y}^{(y)} = \kappa_y^2 n_y(n_y + 2\sigma_y)$, with $\kappa_y = \varrho_y\eta$ and $\sigma_y = \big(a_1^{(y)} + \gamma_y\big)/\eta$.

To obtain the coherent state of the Pöschl–Teller potential, we define the generalizing functional with the form $\mathcal{Z}_{j_y}^{(y)} = \sqrt{f\big(a_1^{(y)}; 2\kappa_y/\eta, \kappa_y\big) f\big(a_1^{(y)}; 2\kappa_y/\eta, 2\kappa_y\big)}$, where $f\big(a_k^{(y)}; c, d\big) = c a_k^{(y)} + d$. It follows that [15]

$$\prod_{k=0}^{n_y-1} \mathcal{Z}_{j_y+k}^{(y)} = \sqrt{\frac{\kappa_y^{2n_y}\Gamma(\nu_y + 2n_y + 1)}{\Gamma(\nu_y+1)}}, \qquad \text{with} \qquad \nu_y = 2a_1^{(y)}/\eta. \tag{60}$$

Assuming $\gamma_y = \eta/2$ and using $e_{n_y}^{(y)}$ and (60) into (30), we find that

$$h_{n_y}^{(y)}\big(a_r^{(y)}\big) = \sqrt{\frac{\Gamma(\nu_y+1)\Gamma(n_y+1)}{\Gamma(\nu_y+n_y+1)}}, \qquad \big|z_y; a_r^{(y)}\big\rangle_y = \sum_{n_y=0}^{\infty}\sqrt{\frac{\Gamma(\nu_y+n_y+1)}{\Gamma(\nu_y+1)\Gamma(n_y+1)}} z_y^{n_y}|n_y\rangle_y. \tag{61}$$

Under these new conditions we identify the partial weights (44) as

$$p_{n_x}^{(x)} = \frac{|z_x|^{2n_x}}{n_x!}, \qquad p_{n_y}^{(y)} = \frac{|z_y|^{2n_y}\Gamma(\nu_y+n_y+1)}{\Gamma(\nu_y+1)\Gamma(n_y+1)}, \tag{62}$$

and obtain the function arguments (45) and (56), and the factors (55) presented in the column HO+PT in table 1. Taking into account the identity [19]

$$\frac{1}{\Gamma(c+1)}\sum_{n=0}^{\infty}\frac{\Gamma(c+n+1)}{\Gamma(n+1)}|z|^{2n} = (1-|z|^2)^{-(c+1)} \tag{63}$$

valid when $|z| < 1$, it is possible to show that the weight distribution function (44) has the form

$$P_{n_x n_y}(z_x, z_y) = \frac{(1-|z_y|^2)^{\nu_y+1}\,\mathrm{e}^{-|z_x|^2}}{\Gamma(\nu_y+1)}\frac{\Gamma(\nu_y+n_y+1)}{\Gamma(n_x+1)\Gamma(n_y+1)}|z_y|^{2n_y}|z_x|^{2n_x}. \tag{64}$$

Figure 3(*a*) shows the population inversion factor $\big\langle\hat{\mathrm{W}}_{\mathrm{U}}^{(\mathrm{X})}(t)\big\rangle$ in terms of the time variable τ_{W} for both models: direct coupled in the top part and conjugate coupled in the bottom part of the figure. We used in these calculations the values $|z_x|^2 = 20$, $|z_y|^2 = 0.75$, $\gamma_x = 1$, $\kappa_y^2 = 0.5$ and $\nu_y = 20$, which were chosen to make evident the collapse and revival phenomenon in the population inversion factor. This application is very illustrative since it makes possible to see in an isolated and different way the action of each coupling potential in the population inversion factor and compare with the results obtained in the case of one coupling potential alone [13]. The sequence of revivals basically shows groups of events modulated with an envelope whose symmetric form is determined for the harmonic oscillator potential. As shown in the insets, each revival event has the basic form characteristic of a Pöschl–Teller potential, discussed in detail in [13], like asymmetric individual envelope and non-periodic Rabi oscillations. Comparing the results obtained with the two models, we verify that the conjugate-coupled model shows a compression in time of the envelope structure of the group of revival events and a deformation in the top part of the envelope of the first revival event. Note the small amplitude observed for the Rabi oscillations.

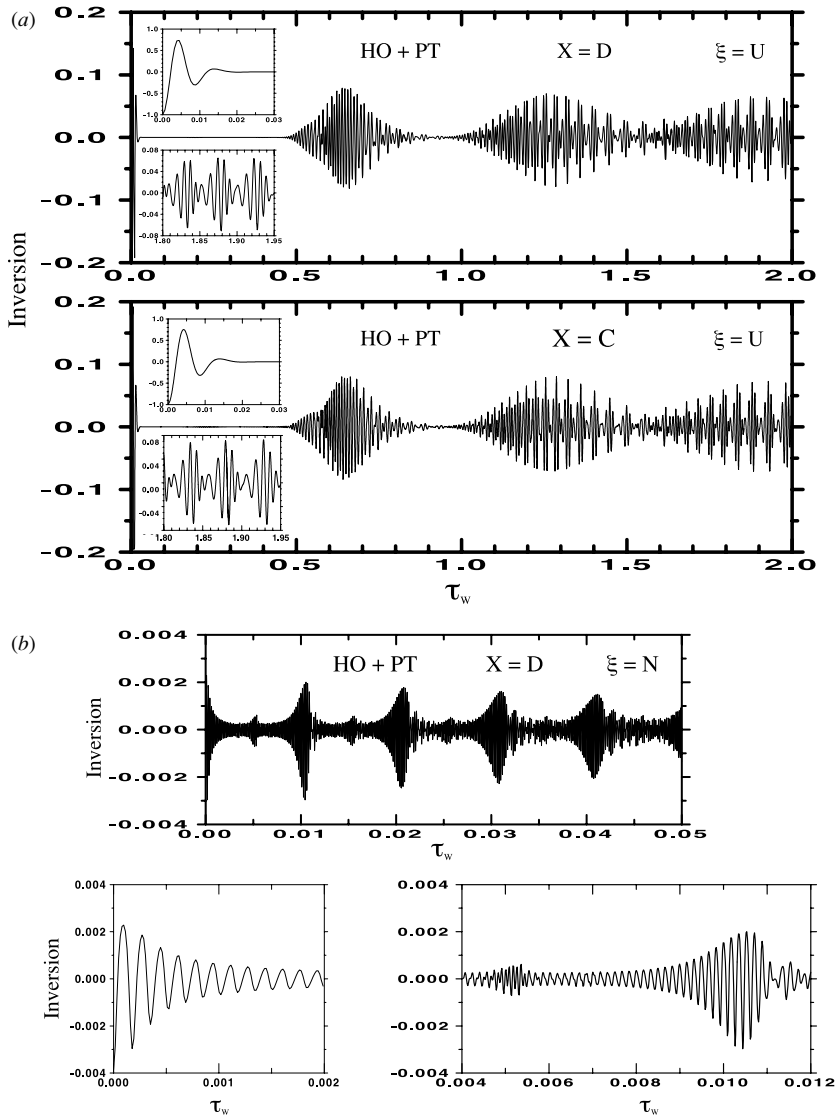

Figure 3. (*a*) Time evolution of the population inversion factor for a harmonic oscillator plus a Pöschl–Teller potential in the direct-coupled model and usual interaction case. The constant values used are $|z_x|^2 = 20$, $|z_y|^2 = 0.75$, $\gamma_x = 1$, $\kappa_y^2 = 0.5$ and $\nu_y = 20$. (*b*) Same as (*a*) for the intensity-dependent interaction case calculated with the strengths $|z_x|^2 = 0.5$, $|z_y|^2 = 0.75$, $\gamma_x = 1$, $\kappa_y^2 = 0.8$ and $\nu_y = 50$.

In figure 3(*b*), we have plotted the population inversion factor $\langle \hat{W}_N^{(D)}(t) \rangle$ in terms of the time variable τ_W calculated with $|z_x|^2 = 0.5$, $|z_y|^2 = 0.75$, $\gamma_x = 1$, $\kappa_y^2 = 0.8$ and $\nu_y = 50$. In this case, reducing the value of $|z_x|^2$ and increasing the value of $|z_y|^2$ allied to the stronger dependence of the cosine function argument in the quantum numbers n_x and n_y, it was possible to change the action of each coupling potential on the results. The sequence of revivals shows groups of events modulated with an envelope whose asymmetric form is basically determined for the Pöschl–Teller potential while, as shown in the insets, each revival event has the basic form characteristic of a harmonic oscillator potential with periodic Rabi oscillations. As a final

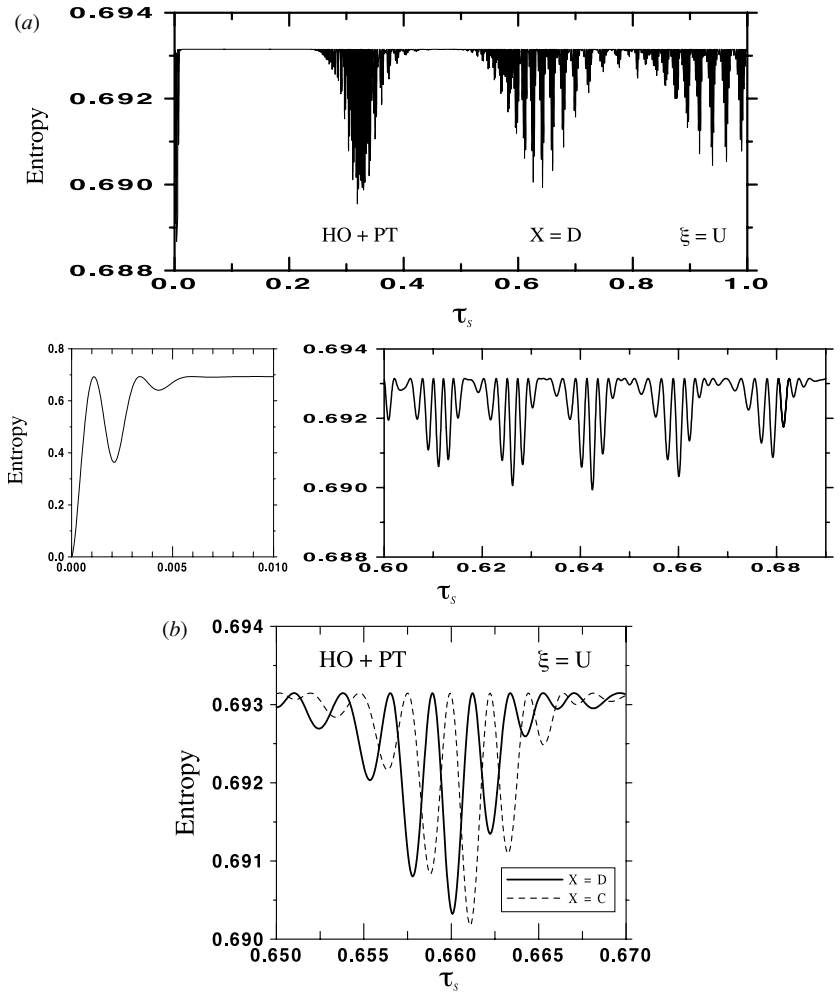

Figure 4. (*a*) Same as figure 3(*a*) for the coupling potentials partial entropy calculated with the same strengths. (*b*) Rabi oscillation packets in the coupling potentials partial entropy for the usual interaction case. The solid line shows the result for the direct-coupled model while the dashed line shows the result for the conjugate-coupled model calculated with the same strengths of figure 3(*a*). (*c*) Same as figure 3(*b*) for the coupling potentials partial entropy calculated with the same strengths.

observation, note the smaller amplitude of the revival events and the absence of a complete collapse in the population inversion factor, since oscillations of very small amplitude survive where we would observe the complete collapse of $\langle \hat{W}_N^{(D)}(t) \rangle$.

In figure 4(*a*), we show the coupling potentials partial entropy $S_P^{(D,U)}(t)$ in terms of the time variable τ_S calculated with the same set of values used in figure 3(*a*). The resemblance in terms of revival events and Rabi oscillations between the behaviour of the two physical quantities is evident, obviously preserving the basic characteristic of each one. Some packets of Rabi oscillation in $S_P^{(D,U)}(t)$ are shown in magnified time views in the bottom part of figure. To have a clearer view of the differences between the results obtained with the two models, in figure 4(*b*) we show as a solid line the fourth group of Rabi oscillation in $S_P^{(D,U)}(t)$ presented in the bottom part of figure 4(*a*). As a dashed line, we have the results obtained for $S_P^{(C,U)}(t)$

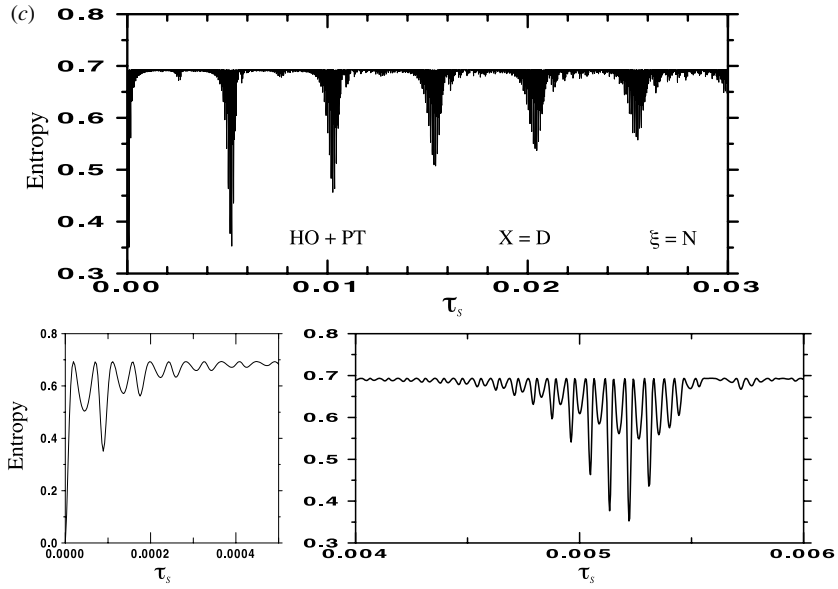

Figure 4. (Continued.)

showing that the basic difference between the two models is a shift in time of the oscillation packets and a reduction in the amplitude of the small oscillation of the borders of the events when X = C.

In figure 4(*c*), we have $S_{\mathrm{P}}^{(\mathrm{D,N})}(\tau_S)$ calculated with the same set of values used in figure 3(*b*). The observations of figure 4(*a*) remain valid now if we compare the behaviour of $\langle \hat{\mathrm{W}}_{\mathrm{N}}^{(\mathrm{D})}(t) \rangle$ and $S_{\mathrm{P}}^{(\mathrm{D,N})}(t)$. In this case, it is interesting to observe that the asymmetry introduced in the envelope of the Rabi oscillations because of the action of the Pöschl–Teller potential makes each packet of the oscillations looks like the superposition of the two independent events with different amplitude envelopes and half of the Rabi frequency (see magnified views in the bottom part of figure).

4.3. Coupling with a harmonic oscillator and a self-similar potentials (HO + sS)

So far, we have only considered examples where the parameters $a_n^{(\alpha)}$ of the partners potentials $V_\alpha^{(\pm)}(\alpha)$ are related by a translation. One class of shape-invariant potentials is given by an infinite chain of reflectionless potentials $V_{k\alpha}^{(\pm)}(\alpha)$ ($k = 0, 1, 2, \ldots$) for which the associated superpotentials $W_\alpha^{(k)}(\alpha)$ satisfy the self-similar ansatz $W_\alpha^{(k)}(\alpha) = q^k W_\alpha^{(k)}(q^k\alpha)$, with $0 < q < 1$. These sets of partner potentials $V_{k\alpha}^{(\pm)}(\alpha)$, also called self-similar (SS) potentials [28], have an infinite number of bound states and their parameters related by a scaling: $a_n^{(\alpha)} = q^{n-1}a_1^{(\alpha)}$, $\forall n \in \mathbb{Z}$. The self-similar potentials can be considered as quantum deformations of the multisoliton solutions corresponding to the Rosen–Morse potential. Indeed working with this kind of potential it is possible to get the Rosen–Morse, harmonic oscillator and Pöschl–Teller potentials as limiting cases [28]. The inclusion of a self-similar potential in the coupling potential system makes possible to evaluate the anharmonic and dissociation effects in the coupled system with a parameter that permits to control these effects and to reduce the results to known ones. In this sense, we assume that the partner potentials (3) for these shape-invariant coupling potential systems are obtained with the superpotentials

$W_x\left(x, a_1^{(x)}\right)$ for a harmonic oscillator, while for the self-similar potential case we have $W_y^{(k)}(y)$. Shape invariance of self-similar potentials was studied in detail in [8]. In the simplest case studied the remainder of equation (4) is given by $R_y\left(a_1^{(y)}\right) = ca_1^{(y)}$, where c is a constant. Using this result in (29) we find $e_{n_y}^{(y)} = R_y\left(a_1^{(y)}\right)\left(1 - q^{n_y}\right)/(1-q)$.

To get a specific form for the coherent state for this coupling potential, we define the generalizing functional as

$$\mathcal{Z}_{j_y}^{(y)} = R_y\left(a_1^{(y)}\right) \qquad \text{so} \qquad \prod_{k=0}^{n_y-1} \mathcal{Z}_{j_y+k}^{(y)} = \left[R_y\left(a_1^{(y)}\right)\right]^{n_y} q^{n_y(n_y-1)/2}. \tag{65}$$

Inserting $e_{n_y}^{(y)}$ and (65) into (30), we can show that

$$h_{n_y}^{(y)}\left(a_r^{(y)}\right) = \rho_y^{-n_y} q^{-n_y^2/4}\sqrt{(q;q)_{n_y}}, \qquad \text{with} \qquad \rho_y = \sqrt{\frac{R_y\left(a_1^{(y)}\right)\{1-q\}}{\sqrt{q}}}. \tag{66}$$

Using these results, we obtain for the coherent state (30) the expression [15]

$$\left|z_y; a_r^{(y)}\right\rangle = \sum_{n_y=0}^{\infty} \frac{q^{n_y^2/4}}{\sqrt{(q;q)_{n_y}}} \beta_y^{n_y} |n_y\rangle_y, \tag{67}$$

where $\beta_y = \rho_y z_y$ and the q-shifted factorial $(q;q)_n$ is defined as $(p;q)_0 = 1$ and $(p;q)_n = \prod_{j=0}^{n-1}(1 - pq^j)$, with $n \in \mathbb{Z}$. Under these new conditions the partial weights (44) are identified as

$$p_{n_x}^{(x)} = \frac{|z_x|^{2n_x}}{n_x!}, \qquad \text{and} \qquad p_{n_y}^{(y)} = \frac{q^{n_y^2/2}|\beta_y|^{2n_y}}{(q;q)_{n_y}}, \tag{68}$$

while the function arguments (45) and (56), and the factors (55) can be determined. The results are shown in the column HO + SS of table 1.

Taking into account the definition of the one-parameter family of q-exponential functions [29, 30]

$$E_q^{(\mu)}(x) = \sum_{n=0}^{\infty} \frac{q^{\mu n^2}}{(q;q)_n} x^n, \qquad \text{with} \quad \mu \in \mathbb{R}, \tag{69}$$

it is possible to show that, in this case, the weight distribution function (44) has the form

$$P_{n_x n_y}(q, z_x, z_y) = \frac{\mathrm{e}^{-|z_x|^2}}{E_q^{(1/2)}(|\beta_y|^2)} \frac{q^{n_y^2/2}}{n_x!(q;q)_{n_y}} |z_x|^{2n_x} |\beta_y|^{2n_y}. \tag{70}$$

If we compare this expression with that one obtained for the pair of harmonic oscillators we observe that (70) looks like the q-version of the double Poissonian distribution (59), with the usual factorial $n_y!$ replaced by the q-shifted factorial $(q;q)_{n_y}$ and the exponential function $\mathrm{e}^{-|z_y|^2}$ replaced by the inverse of the q-exponential function $E_q^{(1/2)}(|\beta_y|^2)$.

Figures 5(*a*)–(*c*) display $\left\langle \hat{\mathrm{W}}_{\mathrm{U}}^{(\mathrm{X})}(\tau_{\mathrm{W}}) \right\rangle$ for both models and the scaling parameter values $q = 0.20, 0.80$ and 0.99, respectively. The set of other values used was $|z_x|^2 = |z_y|^2 = 20$ and $\gamma_x = R_y\left(a_1^{(y)}\right) = 1$. Comparing the time evolution of $\left\langle \hat{\mathrm{W}}_{\mathrm{U}}^{(\mathrm{X})}(\tau_{\mathrm{W}}) \right\rangle$ in this figure the verification of the drastic difference of behaviour obtained with each model is immediate. The revival times for the direct-coupled model are longer than the conjugate-coupled model ones. Besides that the presence of the self-similar coupling potential is almost unperceived in the conjugate-coupled model case since the symmetric envelope and the almost periodic Rabi oscillations are very close to the typical behaviour of a single harmonic oscillator coupled

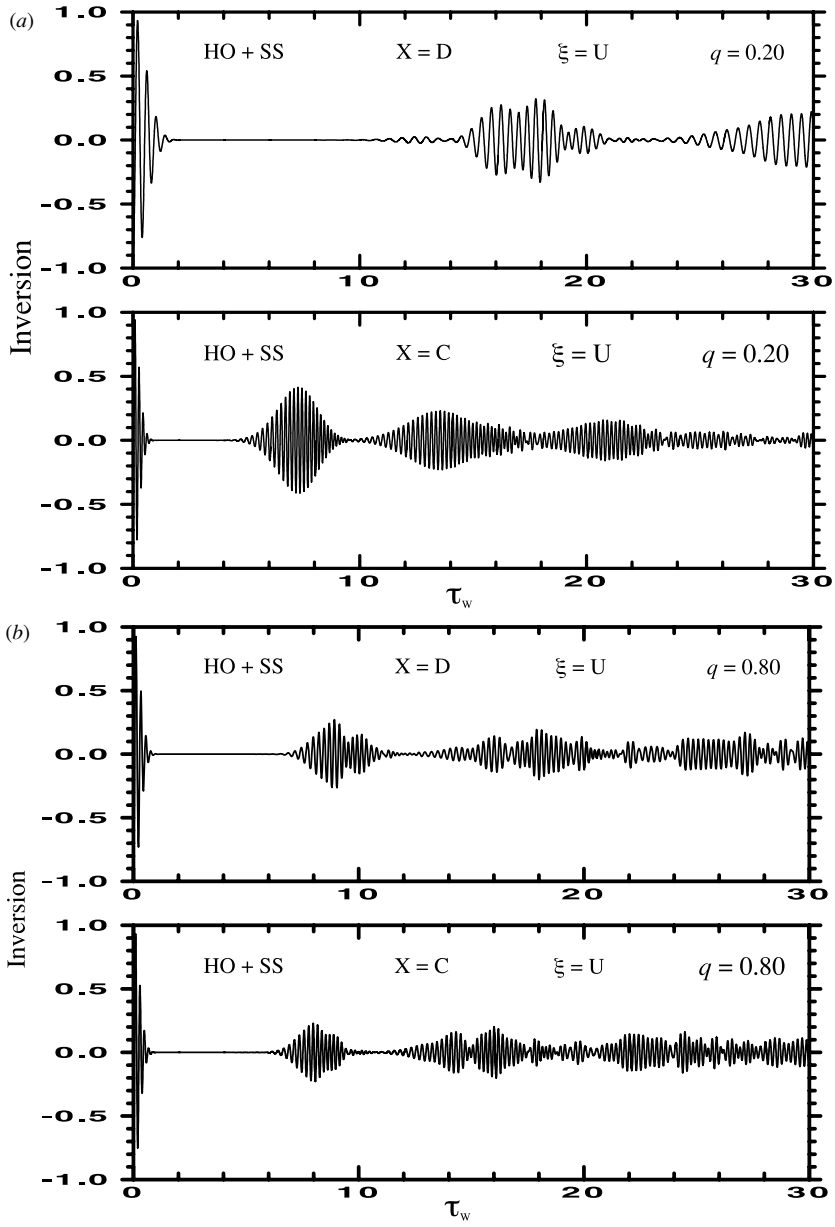

Figure 5. (*a*) Time evolution of the population inversion factor for a harmonic oscillator plus a self-similar potential in the usual interaction case. The top figure shows the result for the direct-coupled model while the bottom figure do the same for the conjugate-coupled model. The constant values used are $|z_x|^2 = |z_y|^2 = 20$, $\gamma_x = R_y(a_1^{(y)}) = 1$ and $q = 0.20$. (*b*) Same as (*a*) for $q = 0.80$. (*c*) Same as (*a*) for $q = 0.99$.

system. Only with a more careful observation, we can perceive the little compression of the Rabi oscillations with the time inside of each revival event. In contrast, for the direct-coupled model the overlapping of three-amplitude different revival events after the first collapse is a clear demonstration of the presence of the two coupling potentials. As we can see in

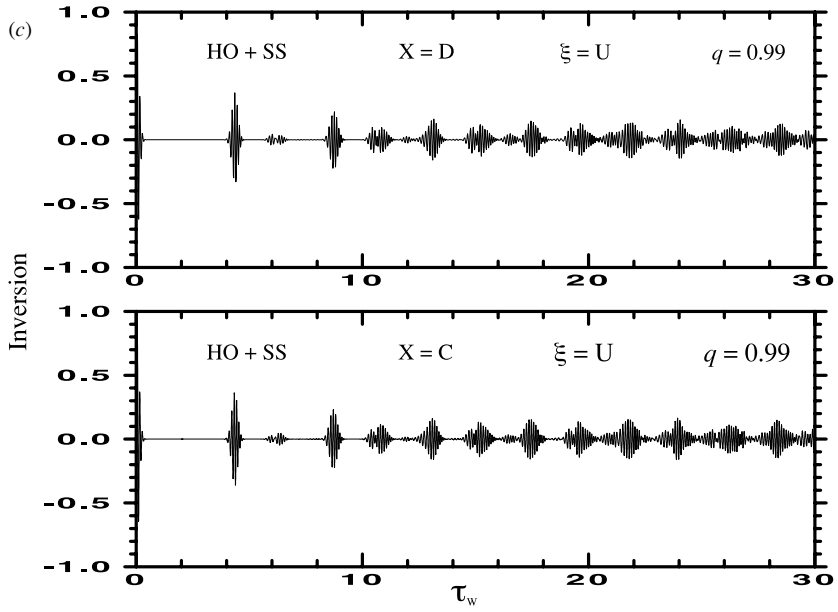

Figure 5. (Continued.)

figures 5(*b*) and (*c*), as soon the scaling parameter q increases the results obtained with the two models tend to a similar behaviour, like the case of a pair of harmonic oscillator coupling potentials presented as our first application. In this sense, we can say that the scaling parameter q can be used as a differentiation factor between the direct-coupled and the conjugate-coupled models when q assumes lower values. Another thing to observe is that for higher values of q the conjugate-coupled model results start to show sensibility to the presence of the two coupling potentials. As a final observation about this set of figures, if we compare the behaviour of $\langle \hat{W}_U^{(X)}(\tau_W) \rangle$ in figure 5(*c*), when $q = 0.99$, and in figure 1(*a*), for a pair of harmonic oscillator coupling potentials, the similarity between the two results for low values of τ_W is evident . In order to understand this tendency we observe that if we take the limit when $q \to 1$ of $e_{n_y}^{(y)}$ and (68) we find that

$$\lim_{q\to 1} e_{n_y}^{(y)} \to n_y R_y\big(a_1^{(y)}\big) \qquad \text{and} \qquad \lim_{q\to 1} p_{n_y}^{(y)} \to \frac{\big|\sqrt{R_y\big(a_1^{(y)}\big)}z_y\big|^{2n_y}}{n_y!}, \tag{71}$$

therefore if we also use the limit [29, 30] $\lim_{q\to 1}\left\{E_q^{(\mu)}[(1-q)\beta]\right\} \to \mathrm{e}^{\beta}$, it is possible to show that

$$\lim_{q\to 1} P_{n_x n_y}(q, z_x, z_y) \longrightarrow \frac{|z_x|^{2n_x}|z_y'|^{2n_y}}{n_x! n_y!}\,\mathrm{e}^{-(|z_x|^2+|z_y'|^2)}, \qquad \text{where} \quad z_y' = R_y\big(a_1^{(y)}\big)z_y, \tag{72}$$

which corresponds to the product of two independent Poisson distributions found for the pair of harmonic oscillator coupling potentials in the first application. This similarity is gradually broken. It happens because for short time intervals the effects of the discrepancy between the value of $q = 0.99$ and the limit $q \to 1$ are less visible than for longer times intervals. Only for q values very close to 1 we will see the exact dynamics of a pair of harmonic oscillator potentials. It is remarkable that in the case of coupling potentials including a self-similar potential, because of the introduction of an additional variable (the scaling parameter q), we

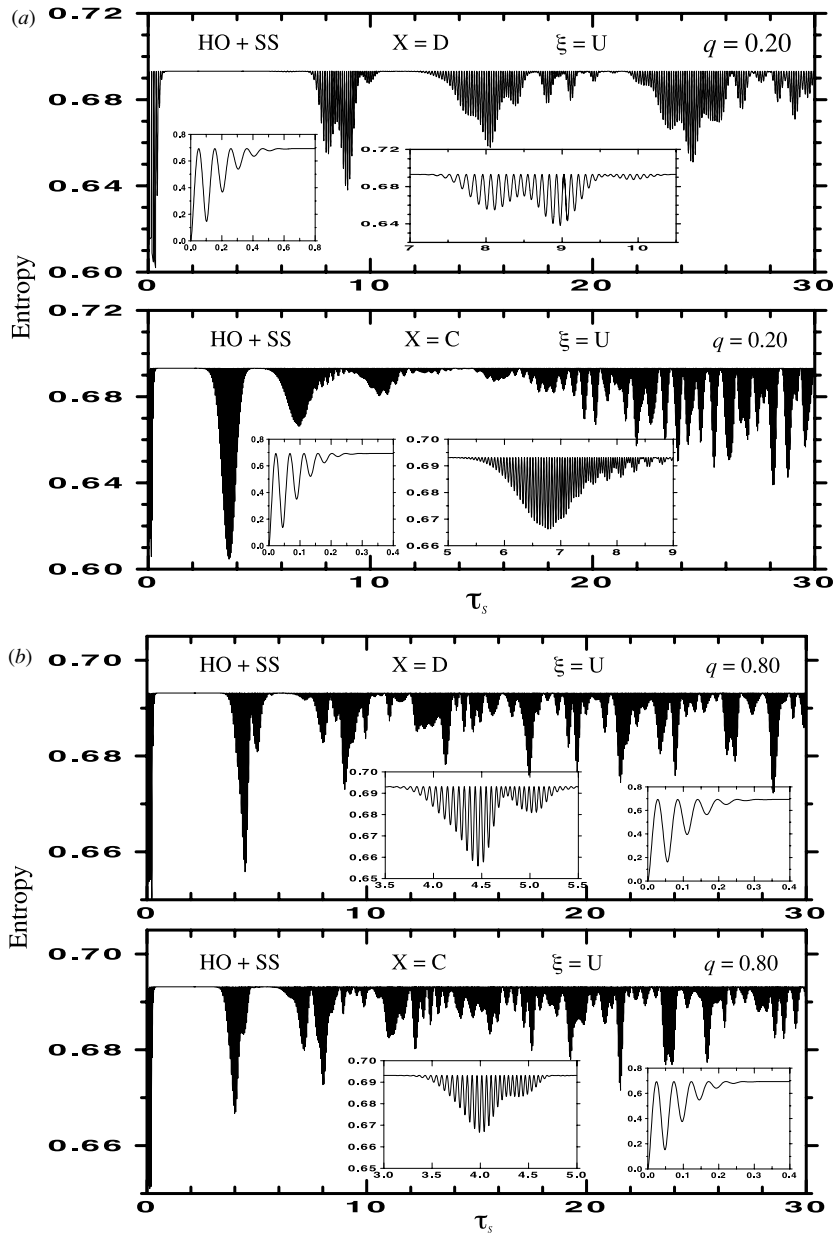

Figure 6. (*a*) Time evolution of the coupling potentials partial entropy for a harmonic oscillator plus a self-similar potential in the usual interaction case. The top figure shows the result for the direct-coupled model while the bottom figure do the same for the conjugate-coupled model calculated with the same strengths of figure 5(*a*). (*b*) Same as (*a*) for $q = 0.80$. (*c*) Same as (*a*) for $q = 0.99$.

have a richer dynamical behaviour with the appearance of new and interesting properties, as shown in [13].

In figures 6(*a*)–(*c*), we show the partial entropy $S_{\mathrm{P}}^{(\mathrm{X,U})}(\tau_S)$ for both models and the scaling parameter values $q = 0.20, 0.80$ and 0.99, respectively. The set of other values used was the

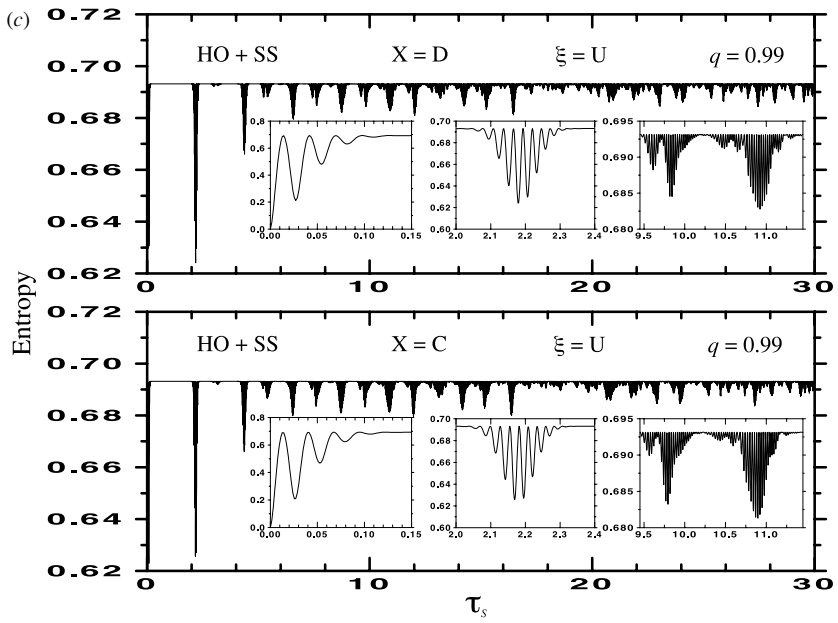

Figure 6. (Continued.)

same as of figures 5. As in the case of the population inversion factor, the results obtained with the two models are very different for lower values of q and tend to an almost similar behaviour in the limit of $q \to 1$. In contrast to $\langle \hat{W}_U^{(C)}(t) \rangle$, the effects of both coupling potentials are also visible in $S_P^{(C,U)}$ when $q = 0.20$, which is traduced with the presence of packets of Rabi oscillations after $8\tau_S$ and the envelope modulating these oscillations. The insets in figure show in detail the first collapse events and some revival events for both models. The observations presented in the inversion population factor remain valid in the case of the coupling potentials partial entropy.

5. Conclusions

Exactly soluble and fully quantum-mechanical models are rare. In the previous paper, we introduced a class of shape-invariant bound-state problems which represents two-level systems coupled with a two-dimensional potential, the independent Cartesian components of which are given by shape-invariant potentials. This is a non-trivial coupled-channels problem which may find applications in molecular, atomic and nuclear physics. Taking into account two possible models (direct- and conjugate-coupled systems) and two possible forms of coupling interaction (usual and intensity-dependent interaction cases), we studied in this paper the quantum dynamics of these models. We determined the density operator of the system and obtained generalized expressions which give the temporal behaviour of the population inversion factor $\langle \hat{W}_\xi^{(X)}(t) \rangle$ as well of the coupling potentials partial entropy $S_P^{(X,\xi)}(t)$. The expressions obtained for these dynamical variables have their behaviour studied for three different kinds of pairs of shape-invariant coupling potentials (two harmonic oscillators, harmonic oscillator + Pöschl–Teller potential and harmonic oscillator + self-similar potential). The results found in these applications exhibit rapid oscillations which periodically collapse and regenerate in different ways depending on the nature of the coupling potentials. Both

collapse and revival events are purely quantum effects resulting from the discreteness of the coupling potential spectra and its initial coherent states form. The action of the two shape-invariant potentials gave rise to a multiplicity of new revival events. On the other hand, for pair of shape-invariant coupling potentials other than two harmonic oscillators, the collapses and revivals show some new and noteworthy properties such as non-regular Rabi oscillation with undefined periods, revivals with asymmetric wing envelopes and increases in the Rabi oscillation numbers. This quantum phenomenon of decay and regeneration is well known in few restricted cases for the population inversion factor when we have harmonic oscillator coupling potentials. Our results confirm that theoretically the occurrence of this interesting quantum phenomenon is not restricted to the population inversion factor but is shared by the other quantum dynamical variables and is related to the model properties, like the kind of interaction and the coherent-states associated with the coupling potentials. It is remarkable that in the case of the self-similar coupling potential we have a wide range of behaviour: the scaling parameter q has a fundamental importance to the dynamical variable since its value defines the complete or incomplete nature of the collapse and revival events. To conclude we observe that, with the use of the partial entropy, this study investigates the influence of the coupling potential forms on the evolution of the quantum correlations (entanglement) between the subsystems that compose the whole coupled system.

Acknowledgments

This work was supported in part by the US National Science Foundation grants no. PHY-0555231 at the University of Wisconsin, and in part by the University of Wisconsin Research Committee with funds granted by the Wisconsin Alumni Research Foundation. ANFA thanks to the Nuclear Theory Group at University of Wisconsin for their very kind hospitality.

References

[1] Aleixo A N F and Balantekin A B 2007 *J. Phys. A: Math. Theor.* **40** 3915
[2] Witten E 1981 *Nucl. Phys.* B **185** 513
for a recent review see Cooper F, Khare A and Sukhatme U 1995 *Phys. Rep.* **251** 267
[3] Gendenshtein L 1983 *Pis'ma Zh. Eksp. Teor. Fiz.* **38** 299
Gendenshtein L 1983 *JETP Lett.* **38** 356
[4] Cooper F, Ginocchio J N and Khare A 1987 *Phys. Rev.* D **36** 2458
[5] Chuan C 1991 *J. Phys. A: Math. Gen.* **24** L1165
[6] Balantekin A B, Cândido Ribeiro M A and Aleixo A N F 1999 *J. Phys. A: Math. Gen.* **32** 2785
[7] Aleixo A N F, Balantekin A B and Cândido Ribeiro M A 2002 *J. Phys. A: Math. Gen.* **35** 9063
[8] Khare A and Sukhatme U 1994 *J. Phys. A: Math Gen.* **26** L901
Barclay D T, Dutt R, Gangopadhyaya A, Khare A, Pagnamenta A and Sukhatme U 1993 *Phys. Rev.* A **48** 2786
[9] Balantekin A B 1998 *Phys. Rev.* A **57** 4188
[10] Chaturvedi S, Dutt R, Gangopadhyay A, Panigrahi P, Rasinariu C and Sukhatme U 1998 *Phys. Lett.* A **248** 109
[11] Aleixo A N F, Balantekin A B and Cândido Ribeiro M A 2000 *J. Phys. A: Math. Gen.* **33** 3173
[12] Aleixo A N F, Balantekin A B and Cândido Ribeiro M A 2001 *J. Phys. A: Math. Gen.* **34** 1109
[13] Aleixo A N F and Balantekin A B 2005 *J. Phys. A: Math. Gen.* **38** 8603
[14] Jaynes E T and Cummings F W 1963 *Proc. IEEE* **51** 89
[15] Aleixo A N F and Balantekin A B 2004 *J. Phys. A: Math. Gen.* **37** 8513
[16] Freitas D S, Vidiella-Barranco A and Roversi J A 1998 *Phys. Lett.* A **249** 275
[17] Buck B and Sukumar C V 1981 *Phys. Lett.* A **81** 132
Buck B and Sukumar C V 1984 *J. Phys. A: Math. Gen.* **17** 885
[18] Eberly J H, Narozhny N B and Sanchez-Mondragon J J 1980 *Phys. Rev. Lett.* **44** 1323
Eberly J H, Narozhny N B and Sanchez-Mondragon J J 1981 *Phys. Rev.* A **23** 236
Yoo H-I, Sanchez-Mondragon J J and Eberly J H 1981 *J. Phys. A: Math. Gen.* **14** 1383
[19] Abramowitz M and Stegun A 1972 *Handbook of Mathematicah Functions* (New York: Dover)

[20] Phoenix S J D and Knight P L 1988 *Ann. Phys.* **186** 381
Phoenix S J D and Knight P L 1988 *Phys. Rev.* A **44** 6023
[21] Shore B W and Knight P L 1993 *J. Mod. Opt.* **40** 1195
[22] von Neumann J 1927 *Mathematical Foundations of Quantum Mechanics 1955* (Princeton, NJ: Princeton University Press)
[23] Araki H and Lieb E H 1970 *Commun. Math. Phys.* **18** 160
[24] Smith D S *Multiple Precision Computation,* home-page: http://myweb.lmu.edu/dmsmith/FMLIB.html; web search keyword: *dsmithfmlibrary*
[25] Klauder J R and Skagerstam B S 1985 *Coherent States—Applications in Physics and Mathemathical Physics* (Singapore: World Scientific)
Perelomov A M 1986 *Generalized Coherent States and Their Applications* (Berlin: Springer)
[26] Gerry C C and Eberly J H 1990 *Phys. Rev.* A **42** 6805
[27] Pöschl G and Teller E 1933 *Z. Phys.* **83** 143
[28] Shabat A B 1992 *Inverse Problem* **8** 303
Spiridonov V 1992 *Phys. Rev. Lett.* **69** 398
[29] Floreanini R, LeTourneux J and Vinet L 1995 *J. Phys. A: Math. Gen.* **28** L287
[30] Atakishiyev N M 1996 *J. Phys. A: Math. Gen.* **29** L223
Exton H 1983 *q-Hypergeometric Functions and Applications* (Chichester: Ellis Horwood)